BEC BIOENERGETICS COMMUNICATIONS

Bioenerg Commun 2020.1
https://doi:10.26124/bec:2020-0001.v1

Consortium communication

Mitochondrial physiology

Gnaiger Erich et al — MitoEAGLE Task Group*

Living Communication *Source:* MitoFit Preprint Arch: doi:10.26124/mitofit:190001.v6
Extended resource of **Mitochondrial respiratory states and rates**

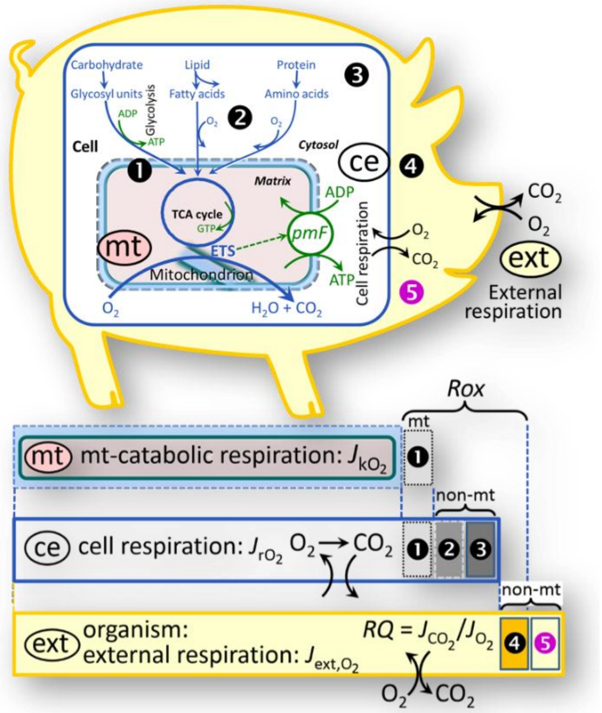

Overview

Internal and external respiration

(mt) **Mitochondrial catabolic respiration** J_{kO_2} is the O_2 consumption in the oxidation of fuel substrates (electron donors) and reduction of O_2 catalysed by the electron transfer system ETS, which drives the protonmotive force *pmF*. J_{kO_2} excludes mitochondrial residual oxygen consumption, mt-*Rox* (❶).

(ce) **Cell respiration** J_{rO_2} is internal cellular O_2 consumption, taking into account all chemical reactions r that consume O_2 in the cells. Catabolic cell respiration is the O_2 consumption associated with catabolic pathways in the cell, including mitochondrial (mt) catabolism, and: mt-*Rox* (❶); non-mt O_2 consumption by catabolic reactions, particularly peroxisomal oxidases and microsomal cytochrome P450 systems (❷); non-mt *Rox* by reactions unrelated to catabolism (❸).

(ext) **External respiration** balances internal respiration at steady state, including extracellular *Rox* (❹) and aerobic respiration by the microbiome (❺).

External O_2 is transported from the environment across the respiratory cascade by circulation between tissues and diffusion across cell membranes, to the intracellular compartment. The respiratory quotient *RQ* is the molar CO_2/O_2 exchange ratio; combined with the nitrogen quotient N/O_2 (mol N given off per mol O_2 consumed), the *RQ* reflects the proportion of carbohydrate, lipid and protein utilized in cell respiration during aerobically balanced steady states. Bicarbonate and CO_2 are transported in reverse to the extracellular milieu and the organismic environment. Hemoglobin provides the molecular paradigm for the combined CO_2/O_2 exchange, as do lungs and gills on the morphological level, but CO_2/O_2 exchange across the skin and other surfaces is less interdependent, and highly independent in cell respiration. Respiratory states are defined in **Table 1**. Rates are illustrated in **Figure 5**. Consult **Tables 4** and **8** for terms, symbols, and units.

Updates:
https://www.bioenergetics-communications.org/index.php/BEC_2020.1_doi10.26124bec2020-0001.v1

Table of contents

Abstract – Executive summary – Box 1: In brief: Mitochondria and bioblasts 2
1.- Introduction 8
2. Coupling states and rates in mitochondrial preparations 8
2.1. Cellular and mitochondrial respiration 8
2.1.1. Aerobic and anaerobic catabolism and ATP turnover

2.1.2. Specification of biochemical dose and exposure
2.2. Mitochondrial preparations 10
2.3. Electron transfer pathways 11
2.4. Respiratory coupling control 12
2.4.1. Coupling
2.4.2. Phosphorylation P» and P»/O_2 ratio
2.4.3. Uncoupling
2.5. Coupling states and respiratory rates 13
2.5.1. LEAK state
2.5.2. OXPHOS state
2.5.3. Electron transfer state
2.5.4. ROX state
2.5.5. Quantitative relations
2.5.6. The steady state
2.6. Classical terminology for isolated mitochondria 19
2.6.1. – 2.6.5. State 1 – State 5
2.7. Control and regulation 21
3. What is a rate? – Box 2: Metabolic flows and fluxes: vectoral, vectorial, and scalar 21
4. Normalization of rate per sample 23
4.1. Flow: per object 23
4.1.1. Count concentration
4.1.2. Flow per single object
4.2. Size-specific flux: per sample size 25
4.2.1. Mass concentration
4.2.2. Size-specific flux
4.3. Marker-specific flux: per mitochondrial content 26
4.3.1. Mitochondrial concentration and mitochondrial density
4.3.2. mt-Marker-specific flux
5. Normalization of rate per system 28
5.1. Flow: per chamber 28
5.2. Flux: per chamber volume 28
5.2.1. System-specific flux
5.2.2. Advancement per volume
6. Conversion of units 30
7. Conclusions – Box 3: Recommendations for studies with mitochondrial preparations 31
References 36
Authors (MitoEAGLE Task Group) – Author contributions 41
Acknowledgements – Competing financial interests – Correspondence

Abstract

As the knowledge base and importance of mitochondrial physiology to evolution, health and disease expands, the necessity for harmonizing the terminology concerning mitochondrial respiratory states and rates has become increasingly apparent. The chemiosmotic theory establishes the mechanism of energy transformation and coupling in oxidative phosphorylation. The unifying concept of the protonmotive force provides the framework for developing a consistent theoretical foundation of mitochondrial physiology and bioenergetics. We follow the latest SI guidelines and those of the International Union of Pure and Applied Chemistry (IUPAC) on terminology in physical chemistry, extended by considerations of open systems and thermodynamics of irreversible processes. The concept-driven constructive terminology incorporates the meaning of each quantity and aligns concepts and symbols with the nomenclature of classical bioenergetics. We endeavour to provide a balanced view of mitochondrial respiratory control and a critical discussion on reporting data of mitochondrial respiration in terms of metabolic flows and fluxes. Uniform standards for evaluation of respiratory states and rates will ultimately contribute

to reproducibility between laboratories and thus support the development of data repositories of mitochondrial respiratory function in species, tissues, and cells. Clarity of concept and consistency of nomenclature facilitate effective transdisciplinary communication, education, and ultimately further discovery.

Keywords—MitoPedia: Respiratory states • SI - The International System of Units • IUPAC • Coupling control • Mitochondrial preparations • Protonmotive force • Uncoupling • Oxidative phosphorylation • Phosphorylation efficiency • Electron transfer pathway • LEAK respiration • Residual oxygen consumption • Normalization of rate • Flow • Flux • Flux control ratio • Mitochondrial marker • Cell count • Oxygen

Executive summary

In view of the broad implications for health care, mitochondrial researchers face an increasing responsibility to disseminate their fundamental knowledge and novel discoveries to a wide range of stakeholders and scientists beyond the group of specialists. This requires implementation of a commonly accepted terminology within the discipline and standardization in the translational context. Authors, reviewers, journal editors, and lecturers are challenged to collaborate with the aim to harmonize the nomenclature in the growing field of mitochondrial physiology and bioenergetics, from evolutionary biology and comparative physiology to mitochondrial medicine. In the present communication we focus on the following concepts in mitochondrial physiology:

1. Aerobic respiration is the O_2 flux in catabolic reactions coupled to phosphorylation of ADP to ATP, and O_2 flux in a variety of O_2 consuming reactions apart from oxidative phosphorylation (OXPHOS). Coupling in OXPHOS is mediated by the translocation of protons across the mitochondrial inner membrane (mtIM) through proton pumps generating or utilizing the protonmotive force that is maintained between the mitochondrial matrix and intermembrane compartment or outer mitochondrial space. Compartmental coupling depends on ion translocation across a semipermeable membrane, which is defined as vectorial metabolism and distinguishes OXPHOS from cytosolic fermentation as counterparts of cellular core energy metabolism (**Overview**). Cell respiration is thus distinguished from fermentation: (*1*) Electron acceptors are supplied by external respiration for the maintenance of redox balance, whereas fermentation is characterized by an internal electron acceptor produced in intermediary metabolism. In aerobic cell respiration, redox balance is maintained by O_2 as the electron acceptor. (*2*) Compartmental coupling in vectorial OXPHOS contrasts to scalar substrate-level phosphorylation in fermentation.

2. When measuring mitochondrial metabolism, the contribution of fermentation and other cytosolic interactions must be excluded from analysis by disrupting the barrier function of the plasma membrane. Selective removal or permeabilization of the plasma membrane yields mitochondrial preparations—including isolated mitochondria, tissue and cell preparations—with structural and functional mitochondrial integrity. Subsequently, extramitochondrial concentrations of oxidizable 'fuel' substrates, as well as ADP, ATP, inorganic phosphate, and cations including H^+ can be controlled to determine mitochondrial function under a set of conditions defined as respiratory states. We strive to incorporate an easily recognized and understood concept-driven terminology of bioenergetics with explicit terms and symbols that define the nature of respiratory states.

3. Mitochondrial coupling states are defined according to the control of respiratory oxygen flux by the protonmotive force *pmF*, in an interaction of the electron transfer system generating the *pmF* and the phosphorylation system utilizing the *pmF*. Capacities of OXPHOS and electron transfer are measured at kinetically-saturating concentrations of fuel substrates, ADP and inorganic phosphate, and O_2, or at optimal uncoupler concentrations, respectively, in

the absence of Complex IV inhibitors such as NO, CO, or H_2S. Respiratory capacity is a measure of the upper limit of the rate of respiration; it depends on the fuel substrate type undergoing oxidation in a mitochondrial pathway, and provides reference values for the diagnosis of health and disease. Evaluation of the impact of evolutionary background, age, gender and sex, lifestyle and environment represents a major challenge for mitochondrial respiratory physiology and pathology.

4. Incomplete tightness of coupling, *i.e.*, some degree of uncoupling relative to the mitochondrial pathway-dependent coupling stoichiometry, is a characteristic of energy-transformations across membranes. Uncoupling or dyscoupling are caused by physiological, pathological, toxicological, pharmacological and environmental conditions that exert an influence not only on the proton leak and cation cycling, but also on proton slip within the proton pumps and the structural integrity of the mitochondria. A more loosely coupled state is induced by stimulation of mitochondrial superoxide formation and the bypass of proton pumps. In addition, the use of protonophores represents an experimental uncoupling intervention to assess the transition from a well-coupled to a noncoupled state of mitochondrial respiration.

5. Respiratory oxygen consumption rates have to be carefully normalized to enable meta-analytic studies beyond the question of a particular experiment. Therefore, all raw data on rates and variables for normalization should be published in an open access data repository. Normalization of rates for: (*1*) the number of objects (cells, organisms); (*2*) the volume or mass of the experimental sample; and (*3*) the concentration of mitochondrial markers in the experimental chamber are sample-specific normalizations, which are distinguished from system-specific normalization for the volume of the experimental chamber (the measuring system).

6. The consistent use of terms and symbols facilitates transdisciplinary communication and will support the further development of a collaborative database on bioenergetics and mitochondrial physiology.

Box 1: In brief – Mitochondria and bioblasts

'For the physiologist, mitochondria afforded the first opportunity for an experimental approach to structure-function relationships, in particular those involved in active transport, vectorial metabolism, and metabolic control mechanisms on a subcellular level' (Ernster and Schatz 1981) [38].

Mitochondria are oxygen-consuming electrochemical generators (**Figure 1**). They evolved from the endosymbiotic alphaproteobacteria which became integrated into a host cell related to Asgard Archaea [85; 72; 117]. Richard Altmann described the 'bioblasts' in 1894 [1], which include not only mitochondria as presently defined, but also symbiotic and free-living bacteria. The word 'mitochondria' (Greek mitos: thread; chondros: granule) was introduced by Carl Benda in 1898 [4]. Mitochondrion is singular and mitochondria is plural. Abbreviation: mt, as generally used in mtDNA.

Contrary to past textbook dogma, which describes mitochondria as individual organelles, mitochondria form dynamic networks within eukaryotic cells. Mitochondrial movement is supported by microtubules. Mitochondrial size and number can change in response to energy requirements of the cell via processes known as fusion and fission; these interactions allow mitochondria to communicate within a network [18]. Mitochondria can even traverse cell boundaries in a process known as horizontal mitochondrial transfer [133]. Another defining morphological characteristic of mitochondria is the double membrane. The mitochondrial inner membrane, mtIM, forms dynamic tubular to disk-shaped cristae that separate the mitochondrial matrix, *i.e.*, the negatively charged internal mitochondrial compartment, from the intermembrane space; the latter being enclosed by the mitochondrial outer membrane, mtOM, and positively charged with respect to the matrix.

Intracellular stress factors may cause shrinking or swelling of the mitochondrial matrix that can ultimately result in permeability transition mtPT [77]. The mtIM contains the non-bilayer phospholipid cardiolipin, which is also involved in the mtOM [47] but is not present in any other eukaryotic cellular membrane. Cardiolipin has many regulatory functions [101]; it promotes and stabilizes the formation of supercomplexes ($SCI_nIII_nIV_n$) based on dynamic interactions between specific respiratory complexes [58; 80; 87], and it supports proton transfer on the mtIM from the electron transfer system to F_1F_0-ATPase (ATP synthase [144]). The mtIM is plastic and exerts an influence on the functional properties of incorporated proteins [135].

Mitochondria constitute the structural and functional elementary components of cell respiration. Aerobic respiration is the reduction of molecular oxygen by electron transfer coupled to electrochemical proton translocation across the mtIM. In the process of OXPHOS, the catabolic reaction sequence of oxygen consumption is electrochemically coupled to the transformation of energy in the phosphorylation of ADP to adenosine triphosphate, ATP [92; 93]. Mitochondria are the powerhouses of the cell that contain the machinery of the OXPHOS pathways, including transmembrane respiratory complexes (proton pumps with FMN, Fe-S and cytochrome *b*, *c*, aa_3 redox systems); alternative dehydrogenases and oxidases; the coenzyme ubiquinone, Q; F_1F_0-ATPase; the enzymes of the tricarboxylic acid cycle, TCA, fatty acid and amino acid oxidation; transporters of ions, metabolites and co-factors; iron/sulphur cluster synthesis; and mitochondrial kinases related to catabolic pathways. TCA cycle intermediates are vital precursors for macromolecule biosynthesis [30]. The mitochondrial proteome comprises over 1200 types of protein [13; 14], mostly encoded by nuclear DNA, nDNA, with a variety of functions, many of which are relatively well known, *e.g.*, proteins regulating mitochondrial biogenesis or apoptosis, while others are still under investigation, or need to be identified, *e.g.*, mtPT pore and alanine transporter. The mammalian mitochondrial proteome can be used to discover and characterize the genetic basis of mitochondrial diseases [102; 142].

Numerous cellular processes are orchestrated by a constant crosstalk between mitochondria and other cellular components. For example, the crosstalk between mitochondria and the endoplasmic reticulum is involved in the regulation of calcium homeostasis, cell division, autophagy, differentiation, and anti-viral signaling [98]. Mitochondria contribute to the formation of peroxisomes, which are hybrids of mitochondrial and ER-derived precursors [131]. Cellular mitochondrial homeostasis (mitostasis) is maintained through regulation at transcriptional, post-translational and epigenetic levels [81; 82], resulting in dynamic regulation of mitochondrial turnover by biogenesis of new mitochondria and removal of damaged mitochondria by fusion, fission and mitophagy [128]. Cell signalling modules contribute to homeostatic regulation throughout the cell cycle or even cell death by activating proteostatic modules, *e.g.*, the ubiquitin-proteasome and autophagy-lysosome/vacuole pathways, specific proteases like LON, and genome stability modules in response to varying energy demands and stress cues [109]. In addition, several post-translational modifications, including acetylation and nitrosylation, are capable of influencing the bioenergetic response, with clinically significant implications for health and disease [17].

Mitochondria of higher eukaryotes typically maintain several copies of their own circular genome known as mitochondrial DNA, mtDNA (hundred to thousands per cell [27]), which is maternally inherited in many species. However, biparental mitochondrial inheritance is documented in some exceptional cases in humans [83], is widespread in birds, fish, reptiles and invertebrate groups, and is even the norm in some bivalve taxonomic groups [9; 140].

The mitochondrial genome of the angiosperm *Amborella* contains a record of six mitochondrial genome equivalents acquired by horizontal transfer of entire genomes, two from angiosperms, three from algae and one from mosses [114]. In unicellular organisms, *i.e.*, protists, the structural organization of mitochondrial genomes is highly variable and includes circular and linear DNA [145]. While some of the free-living flagellates exhibit the largest

Figure 1. Cell respiration and oxidative phosphorylation (OXPHOS)
Mitochondrial respiration is the oxidation of fuel substrates (electron donors) with electron transfer to O_2 as the electron acceptor. For explanation of symbols see also **Overview**.

(a) Respiration of living cells: Extramitochondrial catabolism of macrofuels and uptake of small molecules by the cell provide the mitochondrial fuel substrates. Dashed arrows indicate the connection between the redox proton pumps (respiratory Complexes CI, CIII and CIV) and the transmembrane protonmotive force *pmF*. Coenzyme Q (Q) and the cytochromes *b*, *c*, and aa_3 are redox systems of the mitochondrial inner membrane, mtIM. Glycerol-3-phosphate, Gp.

(b) Respiration in mitochondrial preparations: The mitochondrial electron transfer system ETS is (*1*) fuelled by diffusion and transport of substrates across the mtOM and mtIM, and in addition consists of the (*2*) matrix-ETS, and (*3*) membrane-ETS. Electron transfer converges at the N-junction, and from CI, CII and electron transferring flavoprotein complex CETF at the Q-junction. Unlabeled arrows converging at the Q-junction indicate additional ETS-sections with electron entry into Q through glycerophosphate dehydrogenase, dihydroorotate dehydrogenase, proline dehydrogenase, choline dehydrogenase, and sulfide-ubiquinone oxidoreductase. The dotted arrow indicates the branched pathway of oxygen consumption by alternative quinol oxidase AOX. ET pathways are coupled to the phosphorylation pathway. H^+_{pos}/O_2 shows the ratio of the outward proton flux from the matrix space to the positively (pos) charged vesicular compartment, divided by catabolic O_2 flux in the NADH pathway. The H^+_{neg}/P» ratio is the inward proton flux from the inter-membrane space to the negatively (neg) charged matrix space, divided by the flux of phosphorylation of ADP to ATP. These stoichiometries are not fixed because of ion leaks and proton slip. Moreover, the H^+_{neg}/P» ratio is linked to the F_1F_O-ATPase *c*-ring stoichiometry, which is species-dependent and defines the bioenergetic cost of P». Modified from [78; 116].

(c) OXPHOS-coupling: The H^+ circuit couples O_2 flux J_{kO_2} through the catabolic ET pathway to flux $J_{P»}$ through the phosphorylation pathway converting ADP to ATP.

(d) Phosphorylation pathway catalyzed by the proton pump F_1F_O-ATPase (ATP synthase), adenine nucleotide translocase ANT, and inorganic phosphate carrier PiC. The H^+_{neg}/P» stoichiometry is the sum of the coupling stoichiometry in the F_1F_O-ATPase reaction (-2.7 H^+_{pos} from the positive intermembrane space, 2.7 H^+_{neg} to the matrix, *i.e.*, the negative compartment) and the proton balance in the translocation of ADP^{3-}, ATP^{4-} and P_i^{2-} (negative for substrates). Modified from [54].

known gene coding capacity, *e.g.*, jakobid *Andalucia godoyi* mtDNA codes for 106 genes [12], some protist groups, *e.g.*, alveolates, possess mitochondrial genomes with only three protein-coding genes and two rRNAs [42]. The complete loss of mitochondrial genome is observed in the highly reduced mitochondria of *Cryptosporidium* species [83]. Reaching the final extreme, the microbial eukaryote, oxymonad *Monocercomonoides*, has no mitochondrion whatsoever and lacks all typical nuclear-encoded mitochondrial proteins, showing that while in 99 % of organisms mitochondria play a vital role, this organelle is not indispensable [65].

In vertebrates, but not all invertebrates, mtDNA is compact (16.5 kB in humans) and encodes 13 protein subunits of the transmembrane respiratory Complexes CI, CIII, CIV and ATP synthase (F_1F_O-ATPase), 22 tRNAs, and two ribosomal RNAs. Additional gene content has been suggested to include microRNAs, piRNA, smithRNAs, repeat associated RNA, long noncoding RNAs, and even additional proteins or peptides [23; 35; 74; 111]. The mitochondrial genome requires nuclear-encoded mitochondrially targeted proteins, *e.g.*, TFAM, for its maintenance and expression [110]. The nuclear and the mitochondrial genomes encode peptides of the membrane spanning redox pumps (CI, CIII and CIV) and F_1F_O-ATPase, leading to strong constraints in the coevolution of both genomes [6].

Given the multiple roles of mitochondria, it is perhaps not surprising that mitochondrial dysfunction is associated with a wide variety of genetic and degenerative diseases [41]. Robust mitochondrial function is supported by physical exercise and caloric balance, and is central for sustained

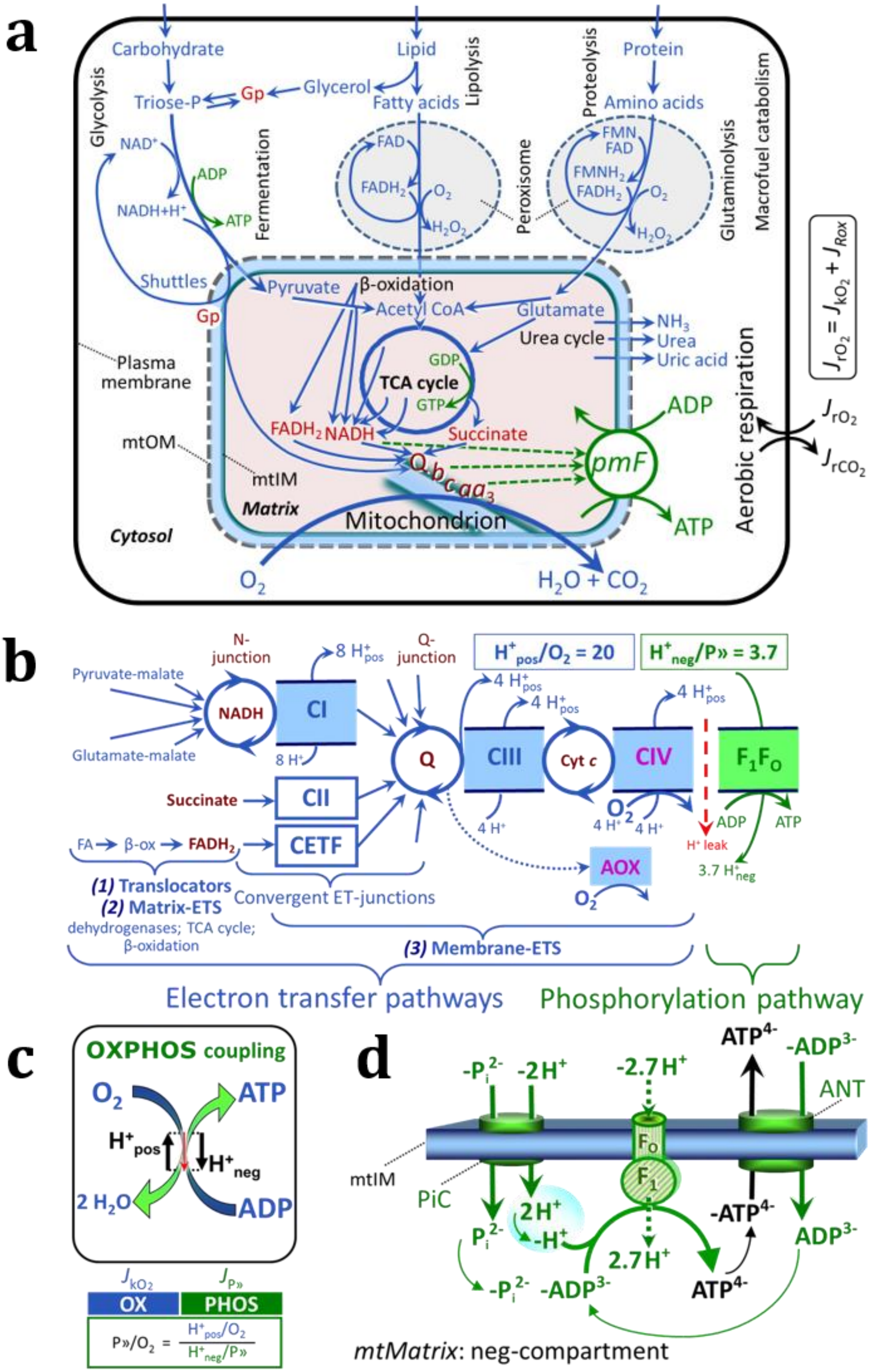
a
Carbohydrate
Lipid
Protein
Glycolysis
Triose-P
Gp
Glycerol
Fatty acids
Lipolysis
Proteolysis
Amino acids
Glutaminolysis
Macrofuel catabolism
NAD+
ADP
NADH+H+
ATP
Fermentation
FAD
FADH2
O2
H2O2
Peroxisome
FMN
FAD
FMNH2
FADH2
O2
H2O2
Shuttles
Pyruvate
β-oxidation
Acetyl CoA
Glutamate
Urea cycle
NH3
Urea
Uric acid
Gp
Plasma membrane
TCA cycle
GDP
GTP
FADH2
NADH
Succinate
ADP
pmF
Q
b
c
aa3
mtOM
mtIM
Matrix
Mitochondrion
Cytosol
ATP
Aerobic respiration
JrO2 = JkO2 + JROX
JrO2
JrCO2
O2
H2O + CO2
b
N-junction
Q-junction
H+pos/O2 = 20
H+neg/P» = 3.7
Pyruvate-malate
Glutamate-malate
NADH
CI
8 H+pos
8 H+
4 H+pos
4 H+pos
4 H+pos
Q
CIII
Cyt c
CIV
F1FO
Succinate
CII
FA
β-ox
FADH2
CETF
4 H+
O2
4 H+
4 H+
ADP
ATP
H+ leak
3.7 H+neg
AOX
O2
(1) Translocators
(2) Matrix-ETS
dehydrogenases; TCA cycle; β-oxidation
Convergent ET-junctions
(3) Membrane-ETS
Electron transfer pathways
Phosphorylation pathway
c
OXPHOS coupling
O2
ATP
H+pos
H+neg
2 H2O
ADP
JkO2
JP»
OX
PHOS
P»/O2 = H+pos/O2 / H+neg/P»
d
-Pi2-
-2H+
-2.7H+
ATP4-
-ADP3-
ANT
Fo
F1
mtIM
PiC
2H+
Pi2-
-H+
2.7H+
-ATP4-
ADP3-
ATP4-
-Pi2-
-ADP3-
mtMatrix: neg-compartment

Figure 1.

metabolic health throughout life. Therefore, a more consistent set of definitions for mitochondrial physiology will increase our understanding of the etiology of disease and improve the diagnostic repertoire of mitochondrial medicine with a focus on protective medicine, evolution, lifestyle, environment, and healthy aging.

1. Introduction

Mitochondria are the powerhouses of the cell with numerous morphological, physiological, molecular, and genetic functions (**Box 1**). Every study of mitochondrial health and disease faces **E**volution, **A**ge, **G**ender and sex, **L**ifestyle, and **E**nvironment (MitoEAGLE) as essential background conditions intrinsic to the individual person or cohort, species, tissue and to some extent even cell line. As a large and coordinated group of laboratories and researchers, the mission of the global MitoEAGLE Network is to generate the necessary scale, type, and quality of consistent data sets and conditions to address this intrinsic complexity. Harmonization of experimental protocols and implementation of a quality control and data management system are required to interrelate results gathered across a spectrum of studies and to generate a rigorously monitored database focused on mitochondrial respiratory function. In this way, researchers from a variety of disciplines can compare their findings using clearly defined and accepted international standards.

With an emphasis on quality of research, published data can be useful far beyond the specific question of a particular experiment. For example, collaborative data sets support the development of open-access databases such as those for National Institutes of Health sponsored research in genetics, proteomics, and metabolomics. Indeed, enabling meta-analysis is the most economic way of providing robust answers to biological questions [25]. However, the reproducibility of quantitative results depend on accurate measurements under strictly-defined conditions. Likewise, meaningful interpretation and comparability of experimental outcomes requires harmonization of protocols between research groups at different institutes. In addition to quality control, a conceptual framework is also required to standardise and harmonise terminology and methodology. Vague or ambiguous jargon can lead to confusion and may convert valuable signals to wasteful noise [100]. For this reason, measured values must be expressed in standard units for each parameter used to define mitochondrial respiratory function. A consensus on fundamental nomenclature and conceptual coherence, however, is missing in the expanding field of mitochondrial physiology. To fill this gap, the present communication provides an in-depth review on harmonization of nomenclature and definition of technical terms, which are essential to improve the awareness of the intricate meaning of current and past scientific vocabulary. This is important for documentation and integration into data repositories in general, and quantitative modelling in particular [3].

In this review, we focus on coupling states and fluxes through metabolic pathways of aerobic energy transformation in mitochondrial preparations in the attempt to establish a conceptually-oriented nomenclature in bioenergetics and mitochondrial physiology in a series of communications, prepared in the frame of the EU COST Action MitoEAGLE open to global bottom-up input.

2. Coupling states and rates in mitochondrial preparations

‘*Every professional group develops its own technical jargon for talking about matters of critical concern ... People who know a word can share that idea with other members of their group, and a shared vocabulary is part of the glue that holds people together and allows them to create a shared culture*’ (Miller 1991) [91].

2.1. Cellular and mitochondrial respiration

2.1.1. Aerobic and anaerobic catabolism and ATP turnover: In respiration, electron transfer is coupled to the phosphorylation of ADP to ATP, with energy transformation mediated by the protonmotive force *pmF* (**Figure 2**). Anabolic reactions are coupled to catabolism, both by ATP as the intermediary energy currency and by small organic precursor molecules as building blocks for biosynthesis [30]. Glycolysis involves substrate-level phosphorylation of ADP to ATP in fermentation without utilization of O_2, studied mainly in living cells and organisms. Many cellular fuel substrates are catabolized to acetyl-CoA or to glutamate, and further electron transfer reduces nicotinamide adenine dinucleotide to NADH or flavin adenine dinucleotide to $FADH_2$. Subsequent mitochondrial electron transfer to O_2 is coupled to proton translocation for the control of the *pmF* and phosphorylation of ADP (**Figure 1b and 1c**). In contrast, extramitochondrial oxidation of odd chain fatty acids, very long chain fatty acids, and some amino acids proceeds partially in peroxisomes without coupling to ATP production: acyl-CoA oxidase catalyzes the oxidation of $FADH_2$ with electron transfer to O_2; amino acid oxidases oxidize flavin mononucleotide $FMNH_2$ or $FADH_2$ (**Figure 1a**).

The plasma membrane separates the intracellular compartment including the cytosol, nucleus, and organelles from the extracellular environment. Cell membranes include the plasma membrane and organellar membranes. The plasma membrane consists of a lipid bilayer with embedded proteins and attached organic molecules that collectively control the selective permeability of ions, organic molecules, and particles across the cell boundary. The intact plasma membrane prevents the passage of many water-soluble mitochondrial substrates and inorganic ions—such as succinate, adenosine diphosphate (ADP) and inorganic phosphate (P_i) that must be precisely controlled at kinetically-saturating concentrations for the analysis of mitochondrial respiratory capacities (**Figure 2**). Respiratory capacities delineate—comparable to channel capacity in information theory [123]—the upper boundary of the rate of O_2 consumption measured in defined respiratory states. The intact plasma membrane limits the scope of investigations into mitochondrial respiratory function in living cells, despite the activity of solute carriers, *e.g.*, the sodium-dependent dicarboxylate transporter SLC13A3 and the sodium-dependent phosphate transporter SLC20A2, which transport specific metabolites across the plasma membrane of various cell types, and the availability of plasma membrane-permeable succinate [37]. These limitations are overcome by the use of mitochondrial preparations.

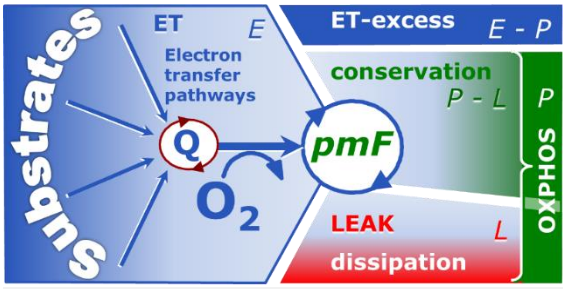

Figure 2. Four-compartment model of oxidative phosphorylation
Respiratory states (ET, OXPHOS, LEAK; **Table 1**) and corresponding rates (*E*, *P*, *L*) are connected by the protonmotive force *pmF*. (*1*) ET capacity *E* is partitioned into (*2*) dissipative LEAK respiration *L*, when the Gibbs energy change of catabolic O_2 flux is irreversibly lost, (*3*) net-OXPHOS capacity (*P-L*), with partial conservation of the capacity to perform work, and (*4*) the ET-excess capacity (*E-P*). Modified from [54].

2.1.2. Specification of biochemical dose and exposure: Substrates, uncouplers, inhibitors, and other chemical reagents are titrated to analyse cellular and mitochondrial function. Nominal concentrations of these substances are usually reported as initial amount of substance concentration c_B [mol·L^{-1}] in the incubation medium.

Kinetically-saturating conditions are evaluated by substrate kinetics to obtain the maximum reaction velocity or maximum pathway flux, in contrast to solubility-saturated conditions. When aiming at the measurement of kinetically-saturated processes—such as OXPHOS capacities—the concentrations for substrates can be chosen according to half-saturating substrate concentrations c_{50}, for metabolic pathways, or the Michaelis constant K_m, for enzyme kinetics. In the case of hyperbolic kinetics, only 80 % of maximum respiratory capacity is obtained at a substrate concentration of four times the c_{50}, whereas substrate concentrations of 5, 9, 19 and 49 times the c_{50} are theoretically required for reaching 83, 90, 95 or 98 % of the maximal rate [51].

Other reagents are chosen to inhibit or alter a particular process. The amount of these chemicals in an experimental incubation is selected to maximize effect, avoiding unacceptable off-target consequences that would adversely affect the data being sought. Specifying the amount of substance in an incubation as nominal concentration in the aqueous incubation medium can be ambiguous [33], particularly for cations (TPP^+; fluorescent dyes such as safranin, TMRM [22]) and lipophilic substances (oligomycin, uncouplers, permeabilization agents [32]), which accumulate in the mitochondrial matrix or on biological membranes, respectively. Generally, dose can be specified per unit of biological sample, *i.e.*, (nominal moles of xenobiotic)/(number of cells) [$mol \cdot x^{-1}$] or, as appropriate, per mass of biological sample [$mol \cdot kg^{-1}$]. This approach to specification of dose provides a scalable parameter that can be used to design experiments, help interpret a wide variety of experimental results, and provide absolute information that allows researchers worldwide to make the most use of published data [33]. Exposure includes the additional dimension of time in contact with a particular dose.

2.2. Mitochondrial preparations

Mitochondrial preparations are defined as either isolated mitochondria or tissue and cell preparations in which the barrier function of the plasma membrane is disrupted. Since this entails the loss of cell viability, mitochondrial preparations are not studied *in vivo*. In contrast to isolated mitochondria and tissue homogenate preparations, mitochondria in permeabilized tissues and cells are *in situ* relative to the plasma membrane. When studying mitochondrial preparations, substrate-uncoupler-inhibitor-titration (SUIT) protocols are used to establish respiratory **C**oupling-**C**ontrol **S**tates (CCS) and **P**athway-**C**ontrol **S**tates (PCS) that provide reference values for various output variables (**Table 1**). Physiological conditions *in vivo* deviate from these experimentally obtained states; this is because kinetically-saturating concentrations, *e.g.,* of ADP, oxygen (O_2; dioxygen) or fuel substrates, may not apply to physiological intracellular conditions. Further information is obtained in studies of kinetic responses to variations in fuel substrate concentrations, [ADP], or [O_2] in the range between kinetically-saturating concentrations and anoxia [51].

The cholesterol content of the plasma membrane is high compared to mitochondrial membranes [70]. Therefore, mild detergents—such as digitonin and saponin—can be applied to selectively permeabilize the plasma membrane via interaction with cholesterol; this allows free exchange of organic molecules and inorganic ions between the cytosol and the immediate cell environment, while maintaining the integrity and localization of organelles, cytoskeleton, and the nucleus. Application of permeabilization agents (mild detergents or toxins) leads to washout of cytosolic marker enzymes—such as lactate dehydrogenase—and results in the complete loss of cell viability (tested by nuclear staining using plasma membrane-impermeable dyes), while mitochondrial function remains intact (tested by cytochrome *c* stimulation of respiration).

Digitonin concentrations have to be optimized according to cell type, particularly since mitochondria from cancer cells contain significantly higher contents of cholesterol in both membranes [2]. For example, a dose of digitonin per cell of 8 $fmol \cdot x^{-1}$ [10 $pg \cdot x^{-1}$; 10 $\mu g \cdot (10^6\ x)^{-1}$] is optimal for permeabilization of endothelial cells, and the concentration in the incubation medium has to be adjusted according to the cell-mass concentration [32]. Respiration of isolated mitochondria remains unaltered after the addition of low concentrations of digitonin or saponin. In addition to mechanical cell disruption during homogenization of tissue, permeabilization agents may be applied to ensure permeabilization of all cells in tissue homogenates.

Suspensions of cells permeabilized in the respiration chamber and crude tissue homogenates contain all components of the cell at highly dilute concentrations. All

Table 1. Coupling states and rates, and residual oxygen consumption in mitochondrial preparations. Respiration- and phosphorylation flux, J_{kO_2} and $J_{P»}$, are rates, characteristic of a state in conjunction with the protonmotive force *pmF*. Coupling states are established at kinetically-saturating concentrations of oxidizable 'fuel' substrates and O_2.

State	Rate	J_{kO_2}	$J_{P»}$	*pmF*	Inducing factors	Limiting factors
LEAK	*L*	low, cation leak-dependent respiration	0	max.	back-flux of cations including proton leak, proton slip	$J_{P»}$ = 0: (*1*) without ADP, *L*(n); (*2*) max. ATP/ADP ratio, *L*(T); or (*3*) inhibition of the phosphorylation pathway, *L*(Omy), *L*(Cat)
OXPHOS	*P*	high, ADP-stimulated respiration, OXPHOS capacity	max.	high	kinetically-saturating [ADP] and [P_i]	ET capacity limits J_{kO_2}, or phosphorylation-pathway capacity limits $J_{P»}$ and in turn J_{kO_2}
ET	*E*	max., noncoupled respiration, ET capacity	0	low	optimal external uncoupler concentration for max. $J_{O_2,E}$	J_{kO_2} by ET capacity
ROX	*Rox*	min., residual O_2 consumption	0	0	$J_{O_2,Rox}$ in non-ET pathway oxidation reactions	inhibition of all ET pathways; or absence of fuel substrates

mitochondria are retained in chemically-permeabilized mitochondrial preparations and crude tissue homogenates. In the preparation of isolated mitochondria, however, the mitochondria are separated from other cell fractions and purified by differential centrifugation, entailing the loss of mitochondria at typical recoveries ranging from 30 to 80 % of total mitochondrial content [71]. Using Percoll or sucrose density gradients to maximize the purity of isolated mitochondria may compromise the mitochondrial yield or structural and functional integrity. Therefore, mitochondrial isolation protocols need to be optimized according to each study. The term *mitochondrial preparation* neither includes living cells, nor submitochondrial particles and further fractionated mitochondrial components.

2.3. Electron transfer pathways

Mitochondrial electron transfer (ET) pathways are fuelled by diffusion and transport of substrates across the mtOM and mtIM. In addition, the mitochondrial electron transfer system ETS consists of the matrix-ETS and membrane-ETS (**Figure 1b**). Upstream sections of ET pathways converge at the NADH-junction (N-junction). NADH is mainly generated in the TCA cycle and is oxidized by Complex I (CI), with further electron entry into the coenzyme Q-junction (Q-junction). Similarly, succinate is formed in the TCA cycle and oxidized by CII to fumarate. CII is part of both the TCA cycle and the ETS, and reduces FAD to $FADH_2$ with further reduction of ubiquinone to ubiquinol downstream of the TCA cycle in the Q-junction. Thus $FADH_2$ is not a substrate but is the product of CII, in contrast to erroneous metabolic maps shown in many publications. β-oxidation of fatty acids FA supplies reducing equivalents via (*1*) $FADH_2$ as the substrate of electron transferring flavoprotein complex CETF; (*2*) acetyl-CoA generated by chain shortening; and (*3*) NADH generated via 3-hydroxyacyl-CoA dehydrogenases. The ATP yield depends on whether acetyl-CoA enters the TCA cycle, or is for example used in ketogenesis.

Selected mitochondrial catabolic pathways of electron transfer from the oxidation of fuel substrates to the reduction of O_2 are stimulated by addition of fuel substrates to the mitochondrial respiration medium after depletion of endogenous substrates (**Figure 1b**). Substrate combinations and specific inhibitors of ET pathway enzymes are used to obtain defined pathway-control states in mitochondrial preparations [54].

2.4. Respiratory coupling control

2.4.1. Coupling: Coupling of electron transfer (ET) to phosphorylation of ADP to ATP is mediated by vectorial translocation of protons across the mtIM. Proton pumps generate or utilize the electrochemical *pmF* (**Figure 1**). The *pmF* is the sum of two partial forces, the electric force (electric potential difference) and chemical force (proton chemical potential difference, related to ΔpH [92; 93]). The catabolic flux of scalar reactions is collectively measured as O_2 flux J_{kO_2}.

Thus mitochondria are elementary components of energy transformation. Energy is a conserved quantity and cannot be lost or produced in any internal process (First Law of Thermodynamics). Open and closed systems can gain or lose energy only by external fluxes—by exchange with the environment. Therefore, energy can neither be produced by mitochondria, nor is there any internal process without energy conservation. Exergy or Gibbs energy ('free energy') is the part of energy that can potentially be transformed into work under conditions of constant temperature and pressure. *Coupling* is the interaction of an exergonic process (spontaneous, negative exergy change) with an endergonic process (positive exergy change) in energy transformations which conserve part of the exergy change. Exergy is not completely conserved, however, except at the limit of 100 % efficiency of energy transformation in a coupled process [49]. The exergy or Gibbs energy change that is not conserved by coupling is irreversibly dissipated, and is accounted for as the entropy change of the surroundings and the system, multiplied by the absolute temperature of the irreversible process [50].

Pathway-control states PCS and coupling-control states CCS are complementary, since mitochondrial preparations depend on (*1*) an exogenous supply of pathway-specific fuel substrates and oxygen, and (*2*) exogenous control of phosphorylation (**Figure 1**).

2.4.2. Phosphorylation P» and P»/O₂ ratio: Phosphorylation in the context of OXPHOS is defined as phosphorylation of ADP by P_i to form ATP. On the other hand, the term phosphorylation is used generally in many contexts, *e.g.*, protein phosphorylation. This provides the argument for introducing a symbol more discriminating and specific than P as used in the P/O ratio (phosphate to atomic oxygen ratio), where P indicates phosphorylation of ADP to ATP or GDP to GTP (**Figure 1**): The symbol P» indicates the endergonic (uphill) direction of phosphorylation ADP→ATP, and likewise P« the corresponding exergonic (downhill) hydrolysis ATP→ADP. P» refers mainly to electrontransfer phosphorylation but may also involve substrate-level phosphorylation as part of the TCA cycle (succinyl-CoA ligase, phosphoglycerate kinase) and phosphorylation of ADP catalyzed by pyruvate kinase, and of GDP phosphorylated by phosphoenolpyruvate carboxykinase. Transphosphorylation is performed by adenylate kinase, creatine kinase (mtCK), hexokinase and nucleoside diphosphate kinase. In isolated mammalian mitochondria, ATP production catalyzed by adenylate kinase (2 ADP ↔ ATP + AMP) proceeds without fuel substrates in the presence of ADP [69]. Kinase cycles are involved in intracellular energy transfer and signal transduction for regulation of energy flux. The P»/O_2 ratio (P»/4 e^-) is two times the 'P/O' ratio (P»/2 e^-). P»/O_2 is a generalized symbol, not specific for reporting P_i consumption (P_i/O_2 flux ratio), ADP depletion (ADP/O_2 flux ratio), or ATP production (ATP/O_2 flux ratio). The mechanistic P»/O_2 ratio—or P»/O_2 stoichiometry—is calculated from the proton–to–O_2 and proton–to–phosphorylation coupling stoichiometries (**Figure 1c**):

$$\text{P»}/O_2 = \frac{H^+_{pos}/O_2}{H^+_{neg}/\text{P»}} \qquad (1)$$

The H^+_{pos}/O_2 coupling stoichiometry (referring to the full four electron reduction of O_2) depends on the relative involvement of the three coupling sites (respiratory Complexes CI, CIII and CIV) in the catabolic ET pathway from reduced fuel substrates (electron donors) to the reduction of O_2 (electron acceptor). This varies with a bypass of: (*1*) CI by single or multiple electron input into the Q-junction; and (*2*) CIV by involvement of alternative oxidases, AOX. AOX are expressed in all plants, some fungi, many protists, and several animal phyla, but are not expressed in vertebrate mitochondria [86].

The H^+_{pos}/O_2 coupling stoichiometry equals 12 in the ET pathways involving CIII and CIV as proton pumps, increasing to 20 for the NADH pathway through CI (**Figure 1b**). A general consensus on H^+_{pos}/O_2 stoichiometries, however, remains to be reached [59; 122; 141]. The $H^+_{neg}/P»$ coupling stoichiometry (3.7; **Figure 1b**) is the sum of 2.7 H^+_{neg} required by the F_1F_O-ATPase of vertebrate and most invertebrate species [138] and the proton balance in the translocation of ADP, ATP and P_i (**Figure 1c**). Taken together, the mechanistic $P»/O_2$ ratio is calculated at 5.4 and 3.3 for the N- and S pathway, respectively (Eq. 1). The corresponding classical P»/O ratios (referring to the 2 electron reduction of 0.5 O_2) are 2.7 and 1.6 [138], in agreement with the measured P»/O ratio for succinate of 1.58 ± 0.02 [57].

2.4.3. Uncoupling: The effective $P»/O_2$ flux ratio ($Y_{P»/O2} = J_{P»}/J_{kO2}$) is diminished relative to the mechanistic $P»/O_2$ ratio by intrinsic and extrinsic uncoupling or dyscoupling (**Figure 3**). This is distinct from switching between mitochondrial pathways that involve fewer than three proton pumps ('coupling sites': Complexes CI, CIII and CIV), bypassing CI through multiple electron entries into the Q-junction, or bypassing CIII and CIV through AOX (**Figure 1b**). Reprogramming of mitochondrial pathways leading to different types of substrates being oxidized may be considered as a switch of gears (changing the stoichiometry by altering the substrate that is oxidized) rather than uncoupling (loosening the tightness of coupling relative to a fixed stoichiometry). In addition, $Y_{P»/O2}$ depends on several experimental conditions of flux control, increasing as a hyperbolic function of [ADP] to a maximum value [51]. Uncoupling of mitochondrial respiration is a general term comprising diverse mechanisms (**Figure 3**):

1. Proton leak across the mtIM from the positive to the negative compartment (H^+ leak-uncoupled);
2. Cycling of other cations, strongly stimulated by mtPT; comparable to the use of protonophores, cation cycling is experimentally induced by valinomycin in the presence of K^+;
3. Decoupling by proton slip in the redox proton pumps (CI, CIII and CIV) when protons are effectively not pumped in the ETS, or are not driving phosphorylation (F_1F_O-ATPase);
4. Loss of vesicular (compartmental) integrity when electron transfer is acoupled;
5. Electron leak in the loosely coupled univalent reduction of O_2 to superoxide ($O_2^{\bullet-}$; superoxide anion radical).

Differences of terms—uncoupled *vs.* noncoupled—are easily overlooked, although they relate to different meanings of uncoupling (**Table 2** and **Figure 3**).

2.5. Coupling states and respiratory rates

To extend the classical nomenclature on mitochondrial respiratory states (Section 2.6) by a concept-driven terminology that explicitly incorporates information on the meaning of respiratory states, the terminology must be general and not restricted to any particular experimental protocol or mitochondrial preparation [53]. Diagnostically meaningful and reproducible conditions are defined for measuring mitochondrial function and respiratory capacities of core energy metabolism. Standard respiratory coupling-control states are obtained while maintaining a defined ET-pathway state with constant fuel substrates and inhibitors of specific branches of the ET pathway. Concept-driven nomenclature aims at mapping the meaning and concept behind the words and acronyms onto the forms of words and acronyms [91]. The focus of concept-driven nomenclature is primarily

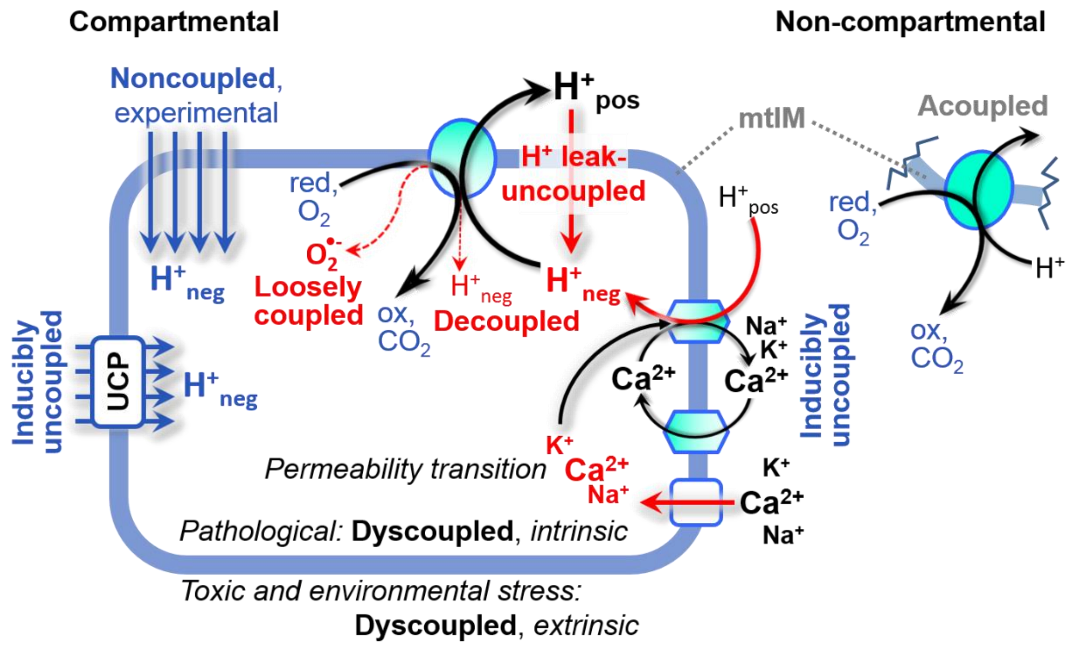

Figure 3. Mechanisms of respiratory uncoupling
An intact mitochondrial inner membrane, mtIM, is required for vectorial, compartmental coupling. Inducible uncoupling, *e.g.*, by activation of UCP1, increases LEAK respiration; experimentally noncoupled respiration provides an estimate of ET capacity obtained by titration of protonophores stimulating respiration to maximum O_2 flux. H^+ leak-uncoupled, decoupled, and loosely coupled respiration are components of intrinsic uncoupling (**Table 2**). Pathological dysfunction may affect all types of uncoupling, including permeability transition mtPT, causing intrinsically dyscoupled respiration. Similarly, toxicological and environmental stress factors can cause extrinsically dyscoupled respiration. 'Acoupled' respiration is the consequence of structural disruption with catalytic activity of non-compartmental mitochondrial fragments. Reduced fuel substrates, red; oxidized products, ox.

the conceptual *why*, along with clarification of the experimental *how* (**Table 1**).

LEAK: The contribution of intrinsically uncoupled O_2 consumption is studied by preventing the stimulation of phosphorylation either in the absence of ADP or by inhibition of the phosphorylation pathway. The corresponding states are collectively classified as LEAK states when O_2 consumption compensates mainly for ion leaks, including the proton leak.

OXPHOS: The ET- and phosphorylation pathways comprise coupled segments of the OXPHOS-system and provide reference values of respiratory capacities. The OXPHOS capacity is measured at kinetically-saturating concentrations of ADP, P_i, fuel substrates and O_2.

ET: Compared to OXPHOS capacity, the oxidative ET capacity reveals the limitation of OXPHOS capacity mediated by the phosphorylation pathway. By application of external uncouplers, ET capacity is measured as noncoupled respiration.

The three coupling states, LEAK, OXPHOS, and ET are shown schematically with the corresponding respiratory rates, abbreviated as *L*, *P*, and *E*, respectively (**Figure 2**). We distinguish between metabolic *pathways* and metabolic *states* with the corresponding metabolic *rates*; for example: ET pathways, ET states, and ET capacities *E*, respectively (**Table 1**). The protonmotive force *pmF* is *maximum* in the LEAK state of coupled mitochondria, driven by LEAK respiration at a minimum back-flux of cations to the matrix side, *high* in the OXPHOS state when it drives phosphorylation, and *very low* in the ET state when uncouplers short-circuit the proton cycle (**Table 1**).

Table 2. Terms on respiratory coupling and uncoupling

	Term	J_{kO_2}	P»/O_2	Notes
intrinsic, no protonophore added	uncoupled	*L*	0	non-phosphorylating LEAK respiration (Fig. 2)
	proton leak-uncoupled		0	component of *L*, H^+ diffusion across the mtIM (Fig. 2b-d)
	inducibly uncoupled		0	by UCP1 or cation (*e.g.,* Ca^{2+}) cycling, strongly stimulated by permeability transition mtPT; experimentally induced by valinomycin in the presence of K^+
	decoupled		0	component of *L*, proton slip when protons are effectively not pumped in the redox proton pumps CI, CIII and CIV or are not driving phosphorylation (F_1F_O-ATPase [16]) (Fig. 2b-d)
	loosely coupled		0	component of *L*, lower coupling due to superoxide formation and bypass of proton pumps by electron leak with univalent reduction of O_2 to superoxide ($O_2^{\bullet-}$; superoxide anion radical)
	dyscoupled		0	mitochondrial dysfunction due to pathologically, toxicologically, environmentally increased uncoupling
	noncoupled	*E*	0	ET capacity, non-phosphorylating respiration stimulated to maximum flux at optimum exogenous protonophore concentration (Fig. 2d)
	well-coupled	*P*	high	OXPHOS capacity, phosphorylating respiration with an intrinsic LEAK component (Fig. 2c)
	fully coupled	*P* – *L*	max.	OXPHOS capacity corrected for LEAK respiration (Fig. 2a)
	acoupled		0	electron transfer in mitochondrial fragments without vectorial proton translocation upon loss of vesicular (compartmental) integrity

2.5.1. LEAK state (**Figure 4a**): The LEAK state is defined as a state of mitochondrial respiration when O_2 flux mainly compensates for ion leaks in the absence of ATP synthesis, at kinetically-saturating concentrations of O_2 and respiratory fuel substrates. LEAK respiration is measured to obtain an estimate of intrinsic uncoupling without addition of an experimental uncoupler: (*1*) in the absence of adenylates, *i.e.*, AMP, ADP and ATP; (*2*) after depletion of ADP at a maximum ATP/ADP ratio; or (*3*) after inhibition of the phosphorylation pathway by inhibitors of F_1F_O-ATPase (oligomycin, Omy) or adenine nucleotide translocase (carboxyatractyloside, Cat). Adjustment of the nominal concentration of these inhibitors to the concentration of biological sample applied can minimize or avoid inhibitory side-effects exerted on ET capacity or even some dyscoupling. The chelator EGTA is added to mt-respiration media to bind free Ca^{2+}, thus limiting cation cycling. The LEAK rate is a function of respiratory state, hence it depends on (*1*) the barrier function of the mtIM ('leakiness'), (*2*) the electrochemical potential differences and concentration differences across the mtIM, and (*3*) the H^+/O_2 ratio of the ET pathway (**Figure 1b**).

- **Proton leak and uncoupled respiration:** The intrinsic proton leak is the *uncoupled* leak current of protons in which protons diffuse across the mtIM in the dissipative direction of the downhill *pmF* without coupling to phosphorylation (**Figure 4a**). The proton leak flux depends non-linearly on the electric membrane potential difference [31; 45], which is a temperature-dependent property of the mtIM and may be enhanced due to possible contamination by free fatty acids. Inducible uncoupling mediated by uncoupling protein 1 (UCP1) is physiologically controlled, *e.g.*, in brown adipose tissue. UCP1 is a member of the mitochondrial carrier family that is involved in the translocation of protons across the mtIM [64]. Consequently, this short-circuit lowers the *pmF* and stimulates electron transfer, respiration, and heat dissipation in the absence of phosphorylation of ADP.

- **Cation cycling:** There can be other cation contributors to leak current including Ca^{2+} and probably magnesium. Ca^{2+} influx is balanced by mitochondrial Na^+/Ca^{2+} or H^+/Ca^{2+} exchange, which is balanced by Na^+/H^+ or K^+/H^+ exchanges. This is another effective uncoupling mechanism different from proton leak (**Table 2**).
- **Proton slip and decoupled respiration:** Proton slip is the *decoupled* process in which protons are only partially translocated by a redox proton pump of the ET pathways and slip back to the original vesicular compartment. The proton leak is the dominant contributor to the overall leak current in mammalian mitochondria incubated under physiological conditions at 37 °C, whereas proton slip increases at lower experimental temperature [16]. Proton slip can also happen in association with the F_1F_O-ATPase, in which the proton slips downhill across the pump to the matrix without contributing to ATP synthesis. In each case, proton slip is a property of the proton pump and increases with the pump turnover rate.
- **Electron leak and loosely coupled respiration**: Superoxide production by the ETS leads to a bypass of redox proton pumps and correspondingly lower $P»/O_2$ ratio. This depends on the actual site of electron leak and the scavenging of superoxide by cytochrome *c*, whereby electrons may re-enter the ETS with proton translocation by CIV.
- **Dyscoupled respiration:** Mitochondrial injuries may lead to *dyscoupling* as a pathological or toxicological cause of *uncoupled* respiration. Dyscoupling may involve any type of uncoupling mechanism, *e.g.*, opening the mtPT pore. Dyscoupled respiration is distinguished from experimentally induced *noncoupled* respiration in the ET state (**Table 2**).
- **Protonophore titration and non-coupled respiration:** Protonophores are uncouplers which are titrated to obtain maximum *noncoupled* respiration as a measure of ET capacity.
- **Loss of compartmental integrity and acoupled respiration:** Electron transfer and catabolic O_2 flux proceed without compartmental proton translocation in disrupted mitochondrial fragments. Such fragments are an artefact of mitochondrial isolation, and may not fully fuse to re-establish structurally intact mitochondria. Loss of mtIM integrity, therefore, is the cause of acoupled respiration, which is a nonvectorial dissipative process without control by the *pmF*.

2.5.2. OXPHOS state (**Figure 4b**): The OXPHOS state is defined as the respiratory state with kinetically-saturating concentrations of ADP and P_i (phosphorylation substrates), respiratory fuel substrates and O_2, in the absence of exogenous uncoupler, to estimate the maximal respiratory capacity in the OXPHOS state for any given ET-pathway state. Respiratory capacities at kinetically-saturating substrate concentrations provide reference values or upper limits of performance, aiming at the generation of data sets for comparative purposes. Physiological activities and effects of substrate kinetics can be evaluated relative to the OXPHOS capacity.

As discussed previously, 0.2 mM ADP does not kinetically-saturate flux in isolated mitochondria [51; 107]; greater [ADP] is required, particularly in permeabilized muscle fibers and cardiomyocytes, to overcome limitations by intracellular

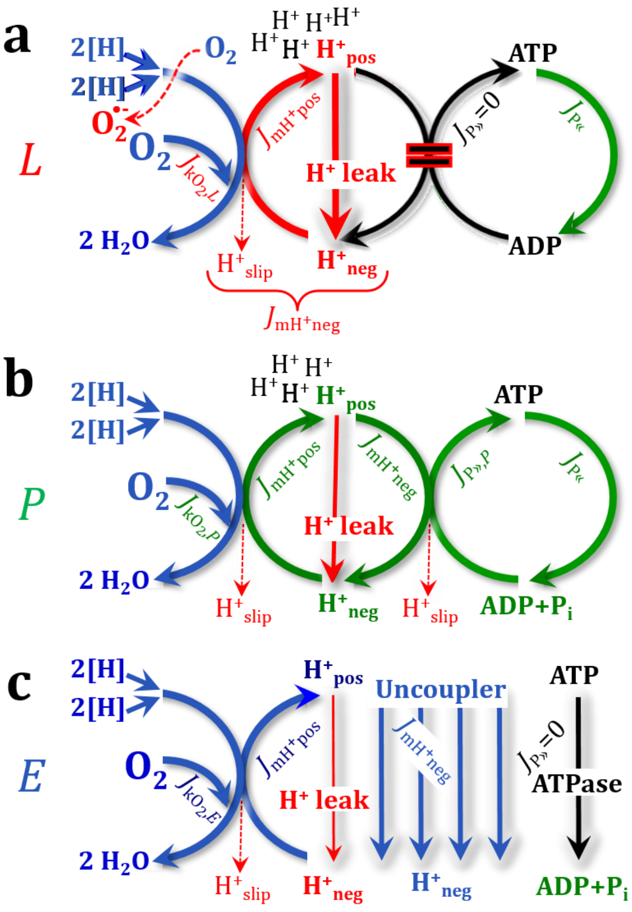

Figure 4. Respiratory coupling states

(a) LEAK state and rate *L*: Oxidation only, since phosphorylation is arrested, $J_{P»}$ = 0, and catabolic O_2 flux $J_{kO_2,L}$ is controlled mainly by the proton leak and slip J_{mH^+neg} (motive, subscript m), at maximum protonmotive force (**Figure 2**). ATP may be hydrolyzed by ATPases, $J_{P«}$; then phosphorylation must be blocked.

(b) OXPHOS state and rate *P*: Oxidation $J_{kO_2,P}$ coupled to phosphorylation $J_{P»,P}$, which is stimulated by kinetically-saturating [ADP] and [P_i]. A high protonmotive force is maintained by pumping of protons J_{mH^+pos} to the positive compartment. O_2 flux $J_{kO_2,P}$ is well-coupled at a P»/O_2 flux ratio of $J_{P»,P}{\cdot}J_{kO_2,P}^{-1}$. Extramitochondrial ATPases may recycle ATP to ADP, $J_{P«}$.

(c) ET state and rate *E*: Oxidation only, since phosphorylation is zero, $J_{P»}$ = 0, at optimum exogenous uncoupler concentration when noncoupled respiration $J_{kO_2,E}$ is maximum. The F_1F_O-ATPase may hydrolyze extramitochondrial ATP translocated into the matrix. Modified from [54].

diffusion and by the reduced conductance of the mtOM [61; 63; 127], either through interaction with tubulin [118] or other intracellular structures [5]. In addition, kinetically-saturating ADP concentrations need to be evaluated under different experimental conditions such as temperature [78] and with different animal models [7]. In permeabilized muscle fiber bundles of high respiratory capacity, the apparent K_m for ADP increases up to 0.5 mM [120], consistent with experimental evidence that >90 % kinetic saturation is reached only at >5 mM ADP [104]. Similar ADP concentrations are also required for accurate determination of OXPHOS capacity in human clinical cancer samples and permeabilized cells [67; 68]. 2.5 to 5 mM ADP is sufficient to obtain the actual OXPHOS capacity in many types of permeabilized tissue and cell preparations, but experimental validation is required in each specific case.

2.5.3. Electron transfer state (Figure 4c):

O_2 flux determined in the ET state yields an estimate of ET capacity. The ET state is defined as the *noncoupled* state with optimum exogenous uncoupler concentration for maximum O_2 flux at kinetically-saturating concentrations of respiratory fuel substrates and O_2. Uncouplers are weak lipid-soluble acids which function as protonophores. These overcome the mtIM barrier function and thus short-circuit the protonmotive system, functioning like a clutch in a mechanical system. As a consequence of the nearly collapsed protonmotive force, the driving force is insufficient for phosphorylation, and $J_{P»}$ = 0. The most frequently used uncouplers are carbonyl cyanide m-chloro phenyl hydrazone (CCCP), carbonyl cyanide *p*-trifluoromethoxyphenylhydrazone (FCCP), or dinitrophenol (DNP). Stepwise titrations of uncouplers stimulate respiration up to or above the level of O_2 consumption rates in the OXPHOS state; respiration is inhibited, however, above optimum uncoupler concentrations [93]. Data obtained with a single dose of uncoupler must be evaluated with caution, particularly when a fixed uncoupler concentration is used in studies exploring a treatment or disease that may alter the mitochondrial content or mitochondrial sensitivity to inhibition by uncouplers. There is a need for new protonophoric uncouplers that drive maximal respiration across a broad dosing range and do not inhibit respiration at high concentrations [66]. The effect on ET capacity of the reversed function of F_1F_O-ATPase ($J_{P«}$; **Figure 4c**) can be evaluated in the presence and absence of extramitochondrial ATP, Omy, or Cat.

2.5.4. ROX state: The state of residual O_2 consumption ROX, is not a coupling state, but is relevant to assess respiratory function (**Overview**). The rate of residual oxygen consumption *Rox* is defined as O_2 consumption due to oxidative reactions measured after inhibition of ET with antimycin A alone, or in combination with rotenone and malonic acid. Cyanide and azide not only inhibit CIV, but also catalase and several peroxidases involved in *Rox*, whereas AOX is not inhibited (**Figure 1b**). High concentrations of antimycin A, but not rotenone or cyanide, inhibit peroxisomal acyl-CoA oxidase and D-amino acid oxidase [134]. *Rox* represents a baseline used to correct respiration measured in defined coupling-control states. *Rox*-corrected *L*, *P* and *E* are not only lower than total fluxes, but also change the flux control ratios *L*/*P* and *L*/*E*. *Rox* is not necessarily equivalent to non-mitochondrial reduction of O_2. This is important when considering O_2-consuming reactions in mitochondria that are not related to ET—such as O_2 consumption in reactions catalyzed by monoamine oxidases (type A and B), monooxygenases (cytochrome P450 monooxygenases), dioxygenases (trimethyllysine dioxygenase), and several hydoxylases. Isolated mitochondrial fractions, especially those obtained from liver, may be contaminated by peroxisomes, as shown by transmission electron microscopy. This fact makes the exact determination of mitochondrial O_2 consumption and mitochondria-associated generation of reactive oxygen species complicated [124; 129] (**Overview**). The variability of ROX-linked O_2 consumption needs to be studied in relation to non-ET enzyme activities, availability of specific substrates, O_2 concentration, and electron leakage leading to the formation of reactive oxygen species.

2.5.5. Quantitative relations: *E* may exceed or be equal to *P*. *E* > *P* is observed in many types of mitochondria, varying between species, tissues and cell types [53]. *E*-*P* is the ET-excess capacity pushing the phosphorylation-flux to the limit of its capacity for utilizing the *pmF* (**Figure 2**). In addition, the magnitude of *E*-*P* depends on the tightness of respiratory coupling or degree of uncoupling, since an increase of *L* causes *P* to increase towards the limit of *E* [79]. The ET-excess capacity *E*-*P*, therefore, provides a sensitive diagnostic indicator of specific injuries of the phosphorylation pathway, under conditions when *E* remains constant but *P* declines relative to controls. Substrate cocktails supporting simultaneous convergent electron transfer to the Q-junction for reconstitution of TCA cycle function establish pathway-control states with high ET capacity, and consequently increase the sensitivity of the *E*-*P* assay.

Theoretically *E* cannot be lower than *P*. *E*<*P* must be discounted as an artefact, which may be caused experimentally by: (*1*) loss of oxidative capacity during the time course of the respirometric assay, since *E* is measured subsequently to *P*; (*2*) using insufficient uncoupler concentrations; (*3*) using high uncoupler concentrations which inhibit ET [52]; (*4*) high oligomycin concentrations applied for measurement of *L* before titrations of uncoupler, when oligomycin exerts an inhibitory effect on *E*. On the other hand, the apparent ET-excess capacity is overestimated if kinetically non-saturating [ADP] or [P_i] are used. See 'State 3' in the next section.

The net OXPHOS capacity is calculated by subtracting *L* from *P*, which requires a cautionary note (**Figure 2**). The net P»/O_2 equals P»/(*P*-*L*), wherein the dissipative LEAK component in the OXPHOS state may be overestimated. This can be avoided by measuring LEAK respiration in a state when the *pmF* is adjusted to its slightly lower value in the OXPHOS state by titration of an ET inhibitor [31]. Any turnover-dependent components of proton leak and slip,

Table 3. Metabolic states of mitochondria (Chance and Williams, 1956; Table V).

State	$[O_2]$	ADP level	Substrate level	Respiration rate	Rate-limiting substance
1	>0	low	low	slow	ADP
2	>0	high	~0	slow	substrate
3	>0	high	high	fast	respiratory chain
4	>0	low	high	slow	ADP
5	0	high	high	0	oxygen

however, are underestimated under these conditions [46]. In general, it is inappropriate to use the term *ATP production* or *ATP turnover* for the difference of O_2 fluxes measured in the OXPHOS- and LEAK states. *P-L* is the upper limit of OXPHOS capacity that is freely available for ATP production (corrected for LEAK respiration) and is fully coupled to phosphorylation with a maximum mechanistic stoichiometry (**Figure 2**).

LEAK respiration and OXPHOS capacity depend on (*1*) the tightness of coupling under the influence of the respiratory uncoupling mechanisms (**Figure 3**), and (*2*) the coupling stoichiometry, which varies as a function of the substrate type undergoing oxidation in ET pathways with either two or three coupling sites (**Figure 1b**). When substrate cocktails are used supporting the convergent NADH- and succinate pathways simultaneously, the relative contribution of ET pathways with three or two coupling sites cannot be controlled experimentally, is difficult to determine, and may shift in transitions between LEAK-, OXPHOS- and ET states [54]. Under these experimental conditions, we cannot separate the tightness of coupling *versus* coupling stoichiometry as the mechanisms of respiratory control in a shift of *L*/*P* ratios. The tightness of coupling and fully coupled O_2 flux (*P-L*; **Table 2**), therefore, are obtained from measurements of coupling control of LEAK respiration, OXPHOS- and ET capacities in well-defined pathway states, using either pyruvate and malate as substrates or the classical succinate and rotenone substrate-inhibitor combination (**Figure 1b**).

2.5.6. The steady state: Mitochondria represent a thermodynamically open system in non-equilibrium states of biochemical energy transformation. State variables (redox states; *pmF*) and metabolic *rates* (fluxes) are measured in defined mitochondrial respiratory *states*. Steady states can be obtained only in open systems, in which changes by internal transformations, *e.g.*, O_2 consumption, are instantaneously compensated for by external fluxes across the system boundary, *e.g.*, O_2 supply, thus preventing a change of O_2 concentration in the system [50]. Mitochondrial respiratory states monitored in closed systems satisfy the criteria of pseudo-steady states for limited periods of time, when changes in the system (concentrations of O_2, fuel substrates, ADP, P_i, H^+) do not exert significant effects on metabolic fluxes (respiration, phosphorylation). Such pseudo-steady states require respiratory media with sufficient buffering capacity and substrates maintained at kinetically-saturating concentrations, and thus depend on the kinetics of the processes under investigation.

2.6. Classical terminology for isolated mitochondria

> *'When a code is familiar enough, it ceases appearing like a code; one forgets that there is a decoding mechanism. The message is identical with its meaning'* (Hofstadter 1979) [60].

Chance and Williams [20; 21] introduced the five classical mitochondrial respiratory and cytochrome redox states. **Table 3** shows a protocol with isolated mitochondria in a closed respirometric chamber, defining a sequence of respiratory states. States and rates are not distinguished in this nomenclature.

2.6.1. State 1 is obtained after addition of isolated mitochondria to air-saturated isoosmotic/isotonic respiration medium containing P_i, but no mitochondrial fuel substrates and no adenylates.

2.6.2. State 2 is induced by addition of a ‘high’ concentration of ADP (typically 100 to 300 µM), which stimulates respiration transiently on the basis of endogenous fuel substrates and phosphorylates only a small portion of the added ADP. State 2 is then obtained at a low respiratory activity limited by exhausted endogenous fuel substrate availability (**Table 3**). If addition of specific inhibitors of respiratory complexes such as rotenone does not cause a further decline of O_2 flux, State 2 is equivalent to the ROX state (**Table 1**). Undefined endogenous fuel substrates are a confounding factor of pathway control, contributing to the effect of subsequently added external substrates and inhibitors. In an alternative sequence of titration steps, the second state (not introduced as State 2) is induced by addition of fuel substrate without ADP or ATP [20, 39]. In contrast to the original State 2 defined in **Table 1** as a ROX state, the alternative ‘State 2’ is a LEAK state, *L*(n). Some researchers have called this condition as ‘pseudostate 4’.

2.6.3. State 3 is the state stimulated by addition of fuel substrates while the ADP concentration in the original State 2 is still high (**Table 3**) and supports coupled energy transformation. 'High ADP' is a concentration of ADP specifically selected to allow the measurement of State 3 to State 4 transitions of isolated mitochondria in a closed respirometric chamber. Repeated ADP titration re-establishes State 3 at ‘high ADP’. Starting at O_2 concentrations near air-saturation (193 or 238 µM O_2 at 37 °C or 25 °C and sea level at 1 atm or 101.32 kPa, and an O_2 solubility of respiration medium at 0.92 times that of pure water [44]), the total ADP concentration added must be low enough (typically 100 to 300 µM) to allow phosphorylation to ATP at a coupled O_2 flux that does not lead to O_2 depletion during the transition to State 4. In contrast, kinetically-saturating ADP concentrations usually are 10-fold higher than 'high ADP', *e.g.,* 2.5 mM in isolated mitochondria. The abbreviation ‘State 3u’ is occasionally used in bioenergetics, to indicate the state of respiration after titration of an uncoupler, without sufficient emphasis on the fundamental difference between OXPHOS capacity (*well-coupled* with an endogenous uncoupled component) and ET capacity (*noncoupled*).

2.6.4. State 4 is a LEAK state that is obtained only if the mitochondrial preparation is intact and well-coupled. Depletion of ADP by phosphorylation to ATP causes a decline of O_2 flux in the transition from State 3 to State 4. Under the conditions of State 4, a maximum protonmotive force and high ATP/ADP ratio are maintained. The gradual decline of $Y_{P»/O_2}$ towards diminishing [ADP] at State 4 must be taken into account for calculation of P»/O_2 ratios [51]. State 4 respiration *L*(T) (**Table 1**), reflects intrinsic proton leak and ATP hydrolysis activity. O_2 flux in State 4 is an overestimation of LEAK respiration if any contaminating ATP hydrolysis activity, $J_{P«}$, recycles some ATP to ADP and thus stimulates respiration coupled to phosphorylation, $J_{P»} > 0$. Some degree of mechanical disruption and loss of mitochondrial integrity allows the exposed mitochondrial F_1F_O-ATPases to hydrolyze the ATP synthesized by the fraction of coupled mitochondria. This can be tested by inhibition of the phosphorylation pathway using oligomycin, ensuring that $J_{P»} = 0$ (State 4o). On the other hand, the State 4 respiration reached after exhaustion of added ADP is a more physiological condition, *i.e.*, presence of ATP, ADP and even AMP. Sequential ADP titrations re-establish State 3, followed by State 3 to State 4 transitions while sufficient O_2 is available. Anoxia may be reached, however, before exhaustion of ADP (State 5).

2.6.5. State 5 ‘*may be obtained by antimycin A treatment or by anaerobiosis*’ [20]. These definitions give State 5 two different meanings: ROX or anoxia. Anoxia is obtained after exhaustion of O_2 in a closed respirometric chamber. Diffusion of O_2 from the surroundings into the aqueous solution may be a confounding factor preventing complete anoxia [51].

In **Table 3**, only States 3 and 4 are coupling-control states, with the restriction that rates in State 3 may be limited kinetically by non-saturating ADP concentrations.

2.7. Control and regulation

The terms metabolic *control* and *regulation* are frequently used synonymously, but are distinguished in metabolic control analysis: '*We could understand the regulation as the mechanism that occurs when a system maintains some variable constant over time, in spite of fluctuations in external conditions (homeostasis of the internal state). On the other hand, metabolic control is the power to change the state of the metabolism in response to an external signal*' [43]. Respiratory control may be induced by experimental control signals that exert an influence on: (*1*) ATP demand and ADP phosphorylation-rate; (*2*) fuel substrate composition, pathway competition; (*3*) available amounts of substrates and O_2, *e.g.*, starvation and hypoxia; (*4*) the protonmotive force, redox states, flux–force relationships, coupling and efficiency; (*5*) Ca^{2+} and other ions including H^+; (*6*) inhibitors, *e.g.*, nitric oxide or intermediary metabolites such as oxaloacetate; (*7*) signalling pathways and regulatory proteins, *e.g.*, insulin resistance, transcription factor hypoxia inducible factor 1.

Mechanisms of respiratory control and regulation include adjustments of: (*1*) enzyme activities by allosteric mechanisms and phosphorylation; (*2*) enzyme content, concentrations of cofactors and conserved moieties such as adenylates, nicotinamide adenine dinucleotide [NAD^+/NADH], coenzyme Q, cytochrome *c*; (*3*) metabolic channeling by supercomplexes; and *(4)* mitochondrial density and morphology (membrane area, cristae folding, fission and fusion). Mitochondria are targeted directly by hormones, *e.g.*, progesterone and glucocorticoids, which affect their energy metabolism [48; 74; 96; 106; 128]. Evolutionary or acquired differences in the genetic and epigenetic basis of mitochondrial function (or dysfunction) between individuals; age; biological sex, and hormone concentrations; life style including exercise and nutrition; and environmental issues including thermal, atmospheric, toxic and pharmacological factors, exert an influence on all control mechanisms listed above. For reviews, see [10; 49; 53; 54; 97; 103].

Lack of control by a metabolic pathway, *e.g.,* phosphorylation pathway, means that there will be no response to a variable activating it, *e.g.,* [ADP]. The reverse, however, is not true as the absence of a response to [ADP] does not exclude the phosphorylation pathway from having some degree of control. The degree of control of a component of the OXPHOS pathway on an output variable, such as O_2 flux, will in general be different from the degree of control on other outputs, such as phosphorylation-flux or proton leak flux. Therefore, it is necessary to be specific as to which input and output are under consideration [43].

Respiratory control refers to the ability of mitochondria to adjust O_2 flux in response to external control signals by engaging various mechanisms of control and regulation. Respiratory control is monitored in a mitochondrial preparation under conditions defined as respiratory states, preferentially under near-physiological conditions of temperature, pH, and medium ionic composition, to generate data of higher biological relevance. When phosphorylation of ADP to ATP is stimulated or depressed, an increase or decrease is observed in electron transfer measured as O_2 flux in respiratory coupling states of intact mitochondria ('controlled states' in the classical terminology of bioenergetics). Alternatively, coupling of electron transfer with phosphorylation is diminished by uncouplers. The corresponding coupling-control state is characterized by a high respiratory rate without control by P» (noncoupled or 'uncontrolled state').

3. What is a rate?

'*Before stating the result of a measurement, it is essential that the quantity being presented is adequately described*' [11]. The term *rate* is not adequately defined to be useful for reporting data. Normalization of rates leads to a diversity of formats expressed in various units. The second [s] is the SI unit for the base quantity *time*. It is also the standard time-unit used in solution chemical kinetics (catalytic activity, unit catal [kat = mol·s^{-1}]).

The inconsistency of the meanings of rate becomes apparent when considering Galileo Galilei's famous principle, that 'bodies of different weight all fall at the same rate (have a constant acceleration)' [26]. A rate may be an extensive quantity [24], which is a *flow I*, when expressed per single object (per elementary entity) or per experimental chamber (system). 'System' is defined as the open or closed experimental chamber in the analytical instrument including a sample s. Alternatively, a rate is a *flux J*, when expressed as a size-specific quantity [50] (**Figure 5a; Box 2**). Importantly, a rate can be a nondimensional *flux control ratio FCR*.

- **Extensive quantities:** An extensive quantity increases proportionally with the size of the object or a system. For example, mass and volume of a sample or system are extensive quantities. Flow is an extensive quantity. The magnitude of an extensive quantity is completely additive for non-interacting subsystems [24].
- **Size-specific quantities:** 'The adjective *specific* before the name of an extensive quantity is often used to mean *divided by mass*' [24]. The term *specific*, however, has different meanings in three particular contexts: (*1*) In the *system*-paradigm, (*a*) mass-specific flux is flow divided by mass of the system (the mass of the entire contents in the experimental chamber or reactor). (*b*) Rates are frequently expressed as volume-specific flux (liquid volume of the experimental chamber). A mass-specific or volume-specific quantity is independent of the extent of non-interacting homogenous subsystems. (*2*) In the context of *sample size*, tissue-specific quantities are related to the mass or volume of the sample in contrast to the mass or volume of the system (*e.g.*, muscle mass-specific or cell volume-specific normalization; **Figure 5**). (*3*) An entirely different meaning of 'specific' is implied in the context of *sample type*, *e.g.*, muscle-specific compared to brain-specific properties.
- **Intensive quantities:** In contrast to size-specific properties, forces are intensive quantities defined as the change of an extensive quantity per advancement of an energy transformation [50].
- **Formats:** Mass m_X can be measured on samples of any type of *X*, but a number of objects N_X and a molar amount n_B can be defined in samples of countable objects only. The molar format is preferred for metabolites including O_2. As of 2019 May 20, the definition of the SI unit mole [mol] is based on a natural constant, namely the Avogadro constant: one mole contains exactly $6.02214076 \cdot 10^{23}$ elementary entities, in contrast to the former definition in terms of the number of molaratoms in the mass of 0.012 kilogram of carbon 12 [11]. Metabolic O_2 flow and flux are expressed in molar units [mol] in biochemistry, but as volume [L] in ergometry. When necessary, these formats can be distinguished as $J_{\underline{n}O_2/m}$ and $J_{\underline{V}O_2/m}$, respectively, indicating the different formats of O_2 in subscripts ($\underline{n}$, $\underline{V}$) with the symbols of the quantities in *underlined italic* font. In many cases it is more practical, however, to use simpler symbols and provide the required definitions in the text and explicitly written units (**Table 4** and **Figure 5**).

Box 2: Metabolic flows and fluxes: vectoral, vectorial, and scalar

Flow is an extensive quantity (*I*; of the system), distinguished from the size-specific quantity flux (*J*; per system size). *Flows* I_{tr} are defined for transformations tr as extensive quantities. This is a generalization derived from electrical terms: Electric charge per unit time is electric flow or current, $I_{el} = dQ_{el} \cdot dt^{-1}$ [A≡ C·s^{-1}]. When dividing I_{el} by size of the system (cross-sectional area of a 'wire'), we obtain flux as a size-specific quantity; this is the current density (surface-density of flow) perpendicular to the direction of flux, $\boldsymbol{J}_{el} = I_{el} \cdot A^{-1}$ [A·m^{-2}] [24]. Fluxes with *spatial* geometric direction and magnitude are *vectors*. Vector and scalar *fluxes* are related to flows as $\boldsymbol{J}_{tr} = I_{tr} \cdot A^{-1}$ [mol·s^{-1}·m^{-2}] and $J_{tr} = I_{tr} \cdot V^{-1}$ [mol·s^{-1}·m^{-3}], expressing flux as an area-specific vector or volume-specific vectorial or scalar quantity,

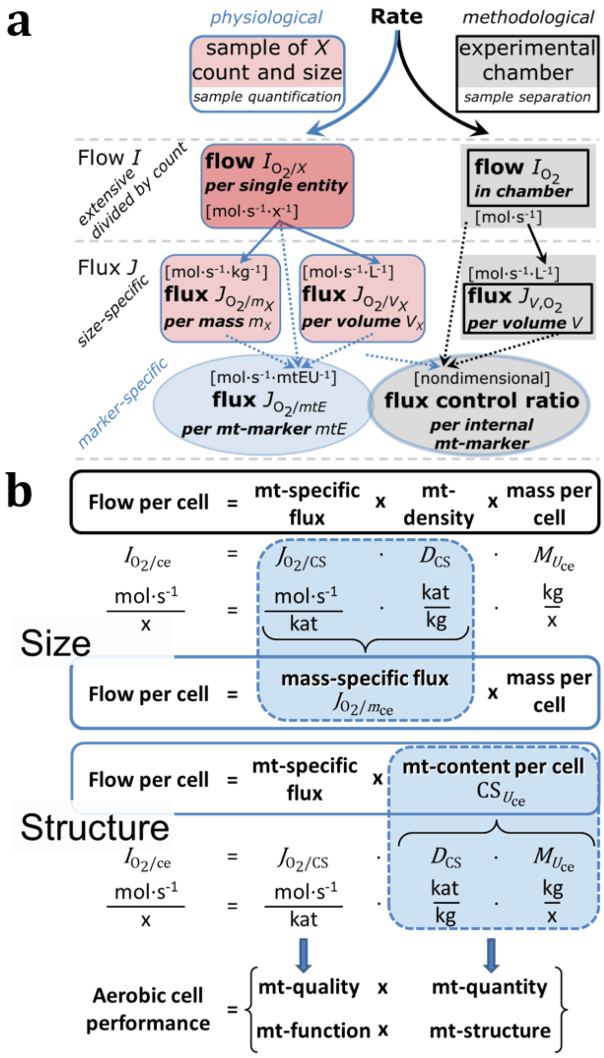

Figure 5. Normalization of rate.

(a) Normalization forms: Left (physiological): Rate can be expressed as extensive *flow* $I_{O2/X}$, if the sample of X can be quantified as a count N_X (X: cell, organism). Rate is a size-specific *flux*, $J_{O2/mX}$ or $J_{O2/VX}$, when expressed per mass or volume of sample of X in the chamber, m_X or V_X. Normalization per mitochondrial elementary marker *mtE* relies on determination of *mtE* expressed in a mt-elementary unit [*mt*EU]. A reference rate can be defined as an internal functional *mtE*, to obtain nondimensional flux control ratios that are independent of sample quantification and even chamber volume. **Right** (methodological): *Flow* in experimental chamber I_{O2}, or *flux* per chamber volume $J_{V,O2}$.

(b) O_2 flow per cell $I_{O2/ce}$: using CS activity as *mtE*, $I_{O2/ce}$ is the product of mt-specific flux $J_{O2/CS}$, mt-density D_{CS}=CS·m_{ce}^{-1}, and mass per cell, $M_{U_{ce}}$=m_{ce}·N_{ce}^{-1}. Then performance is the product of mass-specific flux ($J_{O2/mce}$=$J_{O2/CS}$·D_{ce} [mol·s-1·kg-1]) and *size* (mass per cell $M_{U_{ce}}$ [kg·x-1]), or the product of mitochondrial *function* (mt-specific flux $J_{O2/CS}$) and *structure* (CS per cell, $CS_{U_{ce}}$ =CS·N_{ce}^{-1}). Modified from [54]. See **Tab. 4**.

respectively [50]. We use the meter–kilogram–second–ampere (MKSA) International System of Units (SI) for general cases ([m], [kg], [s] and [A]), with decimal SI prefixes and [L = dm³] for specific applications (**Table 4**).

We suggest defining: (*1*) *vectoral* fluxes, which are translocations as functions of *gradients* with direction in geometric space in continuous systems; (*2*) *vectorial* fluxes, which describe translocations in discontinuous systems and are restricted to information on *compartmental differences* (transmembrane proton flux); and (*3*) *scalar* fluxes, which are localized transformations without translocation, such as chemical reactions or reaction sequences in a homogenous system (catabolic O_2 flux J_{kO2}).

4. Normalization of rate per sample

The challenges of measuring mitochondrial respiratory rate are matched by those of normalization. Normalization is guided by physicochemical principles, methodological considerations, and conceptual strategies (**Table 4**). Normalization per sample concentration is routinely required to report respiratory data (**Figure 5**).

4.1. Flow: per object

4.1.1. Count concentration C_X: The count concentration of objects X is C_X. 'Count' N_X is defined as the 'number of elementary entities' [11]. In the case of animals, N_X is the number of organisms with concentration C_X = N_X·V^{-1} [x·L-1]. Similarly, the number of cells per chamber volume is the cell concentration, where the cell count N_{ce} is the number of cells in the chamber (**Table 4**).

4.1.2. Flow per single object $I_{O2/X}$: O_2 flow per cell is calculated from volume-specific O_2 flux $J_{V,O2}$ [nmol·s-1·L-1] (per V [L] of the experimental system), divided by the

Table 4. Sample concentrations and normalization of flux. SI refers to ref. [11].

Expression	Symbol	Definition	Unit	Notes
Sample	X	sample- or entity-type		1
elementary entity of X; unit X	U_X	single countable object	x	SI; 1, 2
count of X; number of U_X	N_X	$N_X = N \cdot U_X$	x	SI; 2
mass of sample (entity-type X)	m_X		kg	SI; 3
mass per X	M_{U_X}	$M_{U_X} = m_X \cdot N_X^{-1}$	kg·x^{-1}	1, 3
Mitochondria	mt			
mt-elementary entity	mtE		mtEU	
Concentration and density				
molar concentration of X or B	c_X, c_B	$c_B = n_B \cdot V^{-1}$	mol·L^{-1}	SI; 2
count concentration of X	C_X	$C_X = N_X \cdot V^{-1}$	x·L^{-1}	SI; 4
mass concentration of sample	C_{mX}	$C_{mX} = m_X \cdot V^{-1}$	kg·L^{-1}	4
mitochondrial concentration	C_{mtE}	$C_{mtE} = mtE \cdot V^{-1}$	mtEU·L^{-1}	5
mitochondrial density per V_X	D_{mtE/V_X}	$D_{mtE/V_X} = mtE \cdot V_X^{-1}$	mtEU·L^{-1}	6
mitochondrial density per m_X	D_{mtE/m_X}	$D_{mtE/m_X} = mtE \cdot m_X^{-1}$	mtEU·kg^{-1}	6
mitochondrial content per U_X	mtE_{U_X}	$mtE_{U_X} = mtE \cdot N_X^{-1}$	mtEU·x^{-1}	7
O_2 flow and flux				8
flow, system	I_{O_2}	internal flow	mol·s^{-1}	9
volume-specific flux	J_{V,O_2}	$J_{V,O_2} = I_{O_2} \cdot V^{-1}$	mol·s^{-1}·L^{-1}	1, 10
flow per X	$I_{O_2/X}$	$I_{O_2/X} = J_{V,O_2} \cdot C_X^{-1}$	mol·s^{-1}·x^{-1}	11
sample mass-specific flux	J_{O_2/m_X}	$J_{O_2/m_X} = J_{V,O_2} \cdot C_{mX}^{-1}$	mol·s^{-1}·kg^{-1}	1
mt-marker-specific flux	$J_{O_2/mtE}$	$J_{O_2/mtE} = J_{V,O_2} \cdot C_{mtE}^{-1}$	mol·s^{-1}·mtEU^{-1}	12

1 A sample or subsample is one or more parts taken from a study group. A sample of X may contain countable objects. Quantities (N_X, m_X, V_X) that relate to a sample in a mixture are distinguished from quantities for the thermodynamic system (m or V; mass or volume of the total contents in the experimental chamber). See **Table 5** for entity-types X.

2 Entity-type X is indicated by a subscript (N_{ce}; m_{ce}; N_B; V_{O_2}). The elementary entity U_X is count N_X divided by the pure number N. The elementary unit [x] as the unit of count is not in the SI [95]. N_X [x] and n_X [mol] are count and amount of entity-type X; m_X and V_X are count-independent mass and volume of sample-type X, not quantities per U_X (**Table 5**).

3 Units are given in the MKSA system and 1 L=10^{-3} m^3 (**Box 2**). The prefix k is used for the SI base unit of mass (1 kg = 1000 g). Various SI prefixes are used to make numbers easily readable, *e.g.*, 1 mg tissue, cell or mitochondrial mass instead of 0.000 001 kg. The units [kg·x^{-1}] and [kg] distinguish mass per object, M_{U_X} [kg·x^{-1}] (per single cell U_{ce}) from the mass m_{ce} [kg] of a sample of cells that contains any number of cells. For M_{U_X} or $M(U_X)$, the SI uses $m(X)$.

4 IUPAC [24] term: 'number concentration' for C_B. For X = ce, the cell-count concentration is $C_{ce} = N_{ce} \cdot V^{-1}$. $C_{mX} = m_X \cdot V^{-1}$ for sample of X in a mixture. The SI quantity mass density ρ relates to a pure sample S, $\rho = m_S \cdot V_S^{-1}$ (≈1 kg·L^{-1} wet biomass).

5 mt-concentration is the experimental variable of sample concentration in the chamber: (*1*) $C_{mtE} = mtE \cdot V^{-1}$; (*2*) $C_{mtE} = mtE_{U_X} \cdot C_X$; (*3*) $C_{mtE} = D_{mtE/m_X} \cdot C_{mX}$; (*4*) $C_{mtE} = D_{mtE/V_X} \cdot C_{V_X}$

6 For mtE expressed as mt-volume, D_{mtE/V_X} is the mt-volume fraction Φ in sample X(wet). $V_X \approx m_X$, hence $D_{mtE/V_X} \approx D_{mtE/m_X}$.

7 mt-content $mtE_{U_{ce}}$ per single cell equals mtE per cell count N_{ce}, $mtE_{U_{ce}} = mtE \cdot N_{ce}^{-1} = C_{mtE} \cdot C_{ce}^{-1}$.

8 O_2 can be replaced by other chemicals to study different reactions, *e.g.*, ATP, H_2O_2, or vesicular compartmental translocations, *e.g.*, Ca^{2+}.

9 I_{O_2} and V are defined for the experimental system of constant volume (and typically constant temperature), which may be closed or open (**Figure 5**). I_{O_2} is abbreviated for I_{rO_2}, *i.e.*, the metabolic internal O_2 flow of the chemical reaction sequence r in the sample by which O_2 is consumed, with negative stoichiometric number ν_{O_2} = -1: $I_{rO_2} = \mathrm{d_r}n_{O_2}/\mathrm{d}t \cdot \nu_{O_2}^{-1}$. If r includes all reactions in which O_2 participates, then $\mathrm{d_r}n_{O_2} = \mathrm{d}n_{O_2} - \mathrm{d_e}n_{O_2}$, where $\mathrm{d}n_{O_2}$ is the change in the amount of O_2 in the experimental chamber and $\mathrm{d_e}n_{O_2}$ is the amount of O_2 added externally to the system. At steady state in oxystat mode, by definition $\mathrm{d}n_{O_2} = 0$, hence $\mathrm{d_r}n_{O_2} = -\mathrm{d_e}n_{O_2}$. Note that in this context 'external', e, refers to the experimental system, whereas in respiratory physiology 'external', ext, refers to the organism (See **Overview**).

10 Experimental quanity J_{V,O_2}, expressed per volume V of the experimental chamber, equal to V_S for pure samples S only.

11 Flow $I_{O_2/X}$ per elementary entity U_X [mol·s^{-1}·x^{-1}] is a physiological variable normalized for count. It depends on the size (M_{U_X}, V_{U_X}) of U_X. Flow I_{O_2} [mol·s^{-1}] (experimental system) is an experimental variable (Note 9; **Figure 5**).

12 There are many ways to normalize for a mitochondrial marker, that are used in different experimental approaches: (*1*) $J_{O_2/mtE} = J_{V,O_2} \cdot C_{mtE}^{-1}$; (*2*) $J_{O_2/mtE} = J_{V,O_2} \cdot C_{mX}^{-1} \cdot D_{mtE/mX}^{-1} = J_{O_2/mX} \cdot D_{mtE/mX}^{-1}$; (*3*) $J_{O_2/mtE} = J_{V,O_2} \cdot C_X^{-1} \cdot mtE_{U_X}^{-1} = I_{O_2/X} \cdot mtE_{U_X}^{-1}$; (*4*) $J_{O_2/mtE} = I_{O_2} \cdot mtE^{-1}$. The mt-elementary unit [mtEU] varies depending on the mt-marker mtE.

Table 5. Sample preparations and elementary entities, count, mass, and volume

Identity of sample or entity[a] mitochondrial preparation	X	**Unit X** U_X [x]	**Count** N_X [x]	**Mass**[b] m_X [kg]	M_{UX} [kg·x-1]	**Volume**[b] V_X [L]	V_{UX} [L·x-1]
isolated mitochondria	imt	U_{imt}	N_{imt}	m_{imt}	M_{Uimt}	V_{imt}	V_{Uimt}
tissue homogenate	thom			m_{thom}			
permeabilized tissue	pti			m_{pti}			
permeabilized muscle fibers	pfi			m_{pfi}			
permeabilized cells	pce	U_{pce}	N_{pce}	m_{pce}	M_{Upce}	V_{pce}	V_{Upce}
living cells[c]	ce	U_{ce}	N_{ce}	m_{ce}	M_{Uce}	V_{ce}	V_{Uce}
viable cells	vce	U_{vce}	N_{vce}	m_{vce}	M_{Uvce}	V_{vce}	V_{Uvce}
dead cells	dce	U_{dce}	N_{dce}	m_{dce}	M_{Udce}	V_{dce}	V_{Udce}
organisms	org	U_{org}	N_{org}	m_{org}	M_{Uorg}	V_{org}	V_{Uorg}
molecules[d]	B	U_B	N_B	m_B	M_{UB}	V_B	V_{UB}

[a] A sample of X may consist of elementary entities U_X, which are countable objects identified as the defining units U_X.
[b] m_X [kg] and V_X [L] are mass and volume of the sample of X; $M_{U_X} = m_X{\cdot}N_X^{-1}$ [kg·x-1] and $V_{U_X} = V_X{\cdot}N_X^{-1}$ [L·x-1] are quantities per elementary entity U_X (**Table 4**). Wet mass m_w, dry mass m_d, or ash-free dry mass m_{af}, have to be specified [56].
[c] Total cell count in a living cell population, which consists of viable and dead cells, $N_{ce} = N_{vce} + N_{dce}$, without experimental permeabilization of the plasma membrane. Living cells have been called 'intact' cells in contrast to permeabilized cells; but injured cells have lost the property of being intact, yet may still be living.
[d] IUPAC uses for M_{UB} the term 'mass of entity (molecule, formula unit)' with symbol m_f [24], but it should be 'mass per entity', $M_{UB}=m_B{\cdot}N_B^{-1}$. V_B is the volume of molecules B, and the molecular volume is $V_{UB}=V_B{\cdot}N_B^{-1}$ (compare molar volume).

count concentration of cells, $C_{ce} = N_{ce}{\cdot}V^{-1}$. The total cell count is the sum of viable and dead cells, $N_{ce} = N_{vce}+N_{dce}$ (**Table 5**). The cell viability index, $VI_{ce} = N_{vce}{\cdot}N_{ce}^{-1}$, is the ratio of the number of viable cells N_{vce}, per count of all cells in the population. After experimental permeabilization, all cells are permeabilized, $N_{pce} = N_{ce}$. The cell viability index can be used to normalize respiration for the number of cells that have been viable before experimental permeabilization, $I_{O2/vce} = I_{O2/ce}{\cdot}VI^{-1}$, considering that mitochondrial respiratory dysfunction in dead cells might be a confounding factor.

4.2. Size-specific flux: per sample size

4.2.1. Mass concentration C_{mX} [kg·L-1]: Considering permeabilized tissue, homogenate or cells as the sample of X, the sample mass m_X [mg] is frequently measured as wet or dry mass, m_w or m_d [mg], respectively, or as mass of protein $m_{Protein}$. The sample-mass concentration is the mass of the (sub)sample per volume of the experimental system, $C_{mX} = m_X{\cdot}V^{-1}$ [g·L-1 = mg·mL-1]. Sample-types X are isolated mitochondria, tissue homogenate, permeabilized muscle fibers or cells (**Table 4**). m_{ce} [mg] is the total mass *of* all cells X=ce in the experimental system, whereas $M_{Uce} = m_{ce}{\cdot}N_{ce}^{-1}$ [mg·x-1] is the average mass *per* single or unit cell U_{ce} (**Table 5** and **Figure 5**).

4.2.2. Size-specific flux: Cellular O_2 flow can be compared between cells of identical size. To take into account changes and differences in cell size, normalization is required to obtain cell size-specific or mitochondrial marker-specific O_2 flux [113] (**Figure 5**).

- **Sample mass-specific flux $J_{O2/mX}$** [mol·s-1·kg-1]: Sample mass-specific flux is the expression of respiration per mass m_X of a sample of X [mg]. Divide chamber volume-specific flux $J_{V,O2}$ by mass concentration of sample in the chamber, $J_{O2/mX} = J_{V,O2}{\cdot}C_{mX}^{-1}$. Cell mass-specific flux is obtained by dividing flow per unit cell by mass per unit cell, $J_{O2/mX} = I_{O2/X}{\cdot}M_{UX}^{-1}$.
- **Cell volume-specific flux $J_{O2/VX}$** [mol·s-1·L-1]: Sample volume-specific flux is obtained by expressing respiration per volume of sample.

If size-specific O_2 flux is constant and independent of m_X or V_X, then there is no interaction between the subsystems. For example, 1.5 mg and 3.0 mg sub-samples of muscle tissue respire at identical mass-specific flux. If mass-specific O_2 flux, however, changes as a function of the mass of a tissue sample, cells or isolated mitochondria in the experimental chamber, then the nature of the interaction becomes an issue. Therefore, cell concentration must be optimized, particularly in experiments carried out in wells, considering the confluency of the cell monolayer or clumps of cells [121].

The complexity changes when considering the scaling law of respiratory physiology. Strong interactions are revealed between O_2 flow and body mass M of an individual organism: *basal* metabolic rate (flow) does not increase linearly with body mass. *Maximum* mass-specific O_2 flux, $\dot{V}_{O2max}$ or $\dot{V}_{O2peak}$, depends less strongly on individual body mass compared to basal metabolic flux [139]. Individuals, breeds and species deviate substantially from the common scaling relationship. $\dot{V}_{O2peak}$ of human endurance athletes is 60 to 80 mL $O_2 \cdot min^{-1} \cdot kg^{-1}$ body mass, converted to $J_{O2peak/M} = I_{O2peak/org} \cdot M^{-1}$ of 45 to 60 $nmol \cdot s^{-1} \cdot g^{-1}$ [54] (**Table 6**).

4.3. Marker-specific flux: per mitochondrial content

Tissues can contain multiple cell populations that may have distinct mitochondrial subtypes. Mitochondria undergo dynamic fission and fusion cycles, and can exist in multiple stages and sizes that may be altered by a range of factors. The isolation of mitochondria (often achieved through differential centrifugation) can therefore yield a subsample of the mitochondrial types present in a tissue, depending on the isolation protocols utilized. This possible bias should be taken into account when planning experiments using isolated mitochondria. Different sizes of mitochondria are enriched at specific centrifugation speeds, which can be used strategically for isolation of mitochondrial subpopulations.

Part of the mitochondrial content of a tissue is lost during preparation of isolated mitochondria. The fraction of isolated mitochondria obtained from a tissue sample is expressed as mitochondrial recovery. At a high mitochondrial recovery, the fraction of isolated mitochondria is more representative of the total mitochondrial population than in preparations characterized by low recovery. Determination of the mitochondrial recovery and yield is based on measurement of the concentration of a mitochondrial marker in the stock suspension of isolated mitochondria, $C_{mtE,\text{stock}}$, and crude tissue homogenate, $C_{mtE,\text{thom}}$, which together provide information on the mitochondrial density D_{mtE} in the sample (**Table 4**).

When discussing concepts of normalization, it is essential to consider the question posed by the study. If the study aims at comparing tissue performance—such as the effects of a treatment on a specific tissue, then normalization for tissue mass or protein content is appropriate. However, if the aim is to find differences in mitochondrial function independent of mitochondrial density (**Table 4**), then normalization to a mitochondrial marker is imperative (**Figure 5**). One cannot assume that quantitative changes in various markers—such as mitochondrial proteins—necessarily occur in parallel with one another. It should be established that the marker chosen is not selectively altered by the performed treatment. In conclusion, the normalization must reflect the question under investigation to reach a satisfying answer. On the other hand, the goal of comparing results across projects and institutions requires standardization on normalization for entry into a databank.

4.3.1. Mitochondrial concentration C_{mtE} and mitochondrial density D_{mtE}: Mitochondrial organelles compose a dynamic cellular reticulum in various states of fusion and fission. Hence, the definition of a 'number' of mitochondria is often misconceived: mitochondria cannot be counted reliably as a number of occurring elementary particles. Therefore, quantification of mitochondrial concentration and density depends on the measurement of chosen mitochondrial markers. '*Mitochondria are the structural and functional elementary units of cell respiration*' [54]. The quantity of a mitochondrial marker can reflect the total of mitochondrial elementary entities *mtE*, expressed in various mitochondrial elementary units [*mt*EU] specific for each measured mt-marker (**Table 4**). However, since mitochondrial quality may change in response to stimuli—particularly in mitochondrial dysfunction [15], exercise training [105], and aging [29]—some markers can vary while others are unchanged: (*1*) Mitochondrial volume and membrane area are structural markers, whereas mitochondrial protein mass is commonly used as a marker for isolated mitochondria. (*2*) Molecular and enzymatic mitochondrial markers (amounts or activities) can be selected as matrix markers, *e.g.*, citrate synthase activity, mtDNA; mtIM-markers, *e.g.*, cytochrome *c* oxidase activity, aa_3 content, cardiolipin; or mtOM-markers, *e.g.*, the voltage-dependent anion channel (VDAC), TOM20. (*3*) Extending the measurement of mitochondrial marker enzyme activity to mitochondrial pathway capacity, ET- or OXPHOS capacity can be considered as an integrative functional mitochondrial marker.

Depending on the type of mitochondrial marker, the mitochondrial elementary entity *mtE* is expressed in marker-specific units. Mitochondrial concentration C_{mtE} in the experimental chamber and mitochondrial density D_{mtE} in the tissue of origin are quantified as (*1*) the quantity C_{mtE} for normalization in functional analyses, and (*2*) the physiological output D_{mtE} that is the result of mitochondrial biogenesis and degradation, respectively (**Table 4**). It is recommended, therefore, to distinguish *experimental* mitochondrial concentration C_{mtE} in the chamber, and *physiological* mitochondrial density D_{mtE} in the biological sample. The biological variable D_{mtE} is expressed as mitochondrial elementary entities per volume V_X of cells or mass m_X of the sample of *X* (**Figure 5**). The experimental mt-concentration, $C_{mtE} = mtE{\cdot}V^{-1}$ in the chamber volume *V*, is the product of mt-density per mass, $D_{mtE/mX} = mtE{\cdot}m_X^{-1}$, times sample mass concentration, $C_{mX} = m_X{\cdot}V^{-1}$; or C_{mtE} is mt-content, $mtE_{U\mathrm{ce}} = mtE{\cdot}N_{\mathrm{ce}}^{-1}$ per cell, multiplied by cell-count concentration, $C_{\mathrm{ce}} = N_{\mathrm{ce}}{\cdot}V^{-1}$ in the chamber (**Table 4**).

4.3.2. mt-Marker-specific flux $J_{O_2/mtE}$: Volume-specific metabolic O_2 flux depends on: (*1*) the sample concentration in the volume of the experimental chamber, C_{mX} or C_X; (*2*) the mitochondrial density $D_{mtE/VX} = mtE{\cdot}V_X^{-1}$ or content $mtE_{UX} = mtE{\cdot}N_X^{-1}$; and (*3*) the specific mitochondrial activity or performance per mitochondrial elementary marker, $J_{O_2/mtE} = J_{V,O_2}{\cdot}C_{mtE}^{-1}$ [mol·s^{-1}·*mt*EU^{-1}] (**Figure 5**). Obviously, the numerical results and variability of $J_{O_2/mtE}$ vary with the type of mitochondrial marker chosen for measurement of *mtE* and $C_{mtE} = mtE{\cdot}V^{-1}$ [*mt*EU·L^{-1}]. Different methods for the quantification of mitochondrial markers have different strengths and weaknesses. Some problems are common for all mitochondrial markers *mtE*:

(*1*) Accuracy of measurement is crucial, since even a highly accurate and reproducible measurement of chamber volume-specific O_2 flux results in an inaccurate and noisy expression if normalized by a biased and noisy measurement of a mitochondrial marker. This problem is acute in mitochondrial respiration because the denominators used (the mitochondrial markers) are often small moieties of which accurate and precise determination is difficult. In contrast, an *internal* marker is used when O_2 fluxes measured in substrate-uncoupler-inhibitor titration protocols are normalized for flux in a defined respiratory reference state within the assay, which yields flux control ratios *FCR*. *FCR*s are independent of externally measured markers and, therefore, are statistically robust, considering the limitations of ratios in general [62]. *FCR*s indicate qualitative changes of mitochondrial respiratory control, with highest quantitative resolution, separating the effect of mitochondrial density on $J_{O_2/mX}$ and $I_{O_2/X}$ from that of function per mitochondrial elementary marker, $J_{O_2/mtE}$ [54; 105].

(*2*) If mitochondrial quality does not change and only the amount of mitochondria varies as a determinant of mass-specific flux, any marker is equally qualified in principle; then in practice selection of the optimum marker depends only on the accuracy and precision of measurement of the mitochondrial marker.

(*3*) If mitochondrial flux control ratios change, then there may not be any best mitochondrial marker. In general, measurement of multiple mitochondrial markers enables a comparison and evaluation of normalization for these mitochondrial markers. Particularly during postnatal development, the activity of marker enzymes—such as cytochrome *c* oxidase and citrate synthase—follows different time courses [34]. Evaluation of mitochondrial markers in healthy controls is insufficient for providing guidelines for application in the diagnosis of pathological states and specific treatments [125].

In line with the concept of the respiratory acceptor control ratio *RCR* [19], the most readily applied normalization is that of flux control ratios and flux control factors [53; 54]. Then, instead of a specific mt-enzyme activity, the respiratory rate in a reference state serves as the *mtE*, yielding a nondimensional ratio of two fluxes measured consecutively in the same respirometric titration protocol. Selection of the state of maximum flux in a protocol as the reference state — *e.g.*, ET state in L/E and P/E flux control ratios [53] — has the advantages of: (*1*) elimination of experimental variability in additional measurements, such as determination of enzyme activity or tissue mass; (*2*) statistically validated linearization of the response in the range of 0 to 1; and (*3*) consideration of maximum flux for integrating a large number of metabolic steps in the OXPHOS- or ET pathways. This reduces the risk of selecting a functional marker that is specifically altered by the treatment or pathology, yet increases the chance that the highly integrative pathway is disproportionately affected, *e.g.,* the OXPHOS- rather than ET pathway in case of an enzymatic defect in the phosphorylation pathway. In this case, additional information can be obtained by reporting flux control ratios based on a reference state that indicates stable tissue mass-specific flux [125].

Stereological measurement of mitochondrial content via two-dimensional transmission electron microscopy is considered as the gold standard in determination of mitochondrial volume fractions in cells and tissues [139]. Accurate determination of three-dimensional volume by two-dimensional microscopy, however, is both time consuming and statistically challenging [73]. The validity of using mitochondrial marker enzymes (citrate synthase activity, CI to CIV amount or activity) for normalization of flux is limited in part by the same factors that apply to flux control ratios. Strong correlations between various mitochondrial markers and citrate synthase activity [8; 94; 112] are expected in a specific tissue of healthy persons and in disease states not specifically targeting citrate synthase. Citrate synthase activity is acutely modifiable by exercise [76; 132]. Evaluation of mitochondrial markers related to a selected age and sex cohort cannot be extrapolated to provide recommendations for normalization in respirometric diagnosis of disease, in different states of development and aging, different cell types, tissues, and species. mtDNA normalized to nDNA via qPCR is correlated to functional mitochondrial markers including OXPHOS- and ET capacity in some cases [8; 36; 88; 108; 137], but lack of such correlations have been reported [90; 105; 126]. Several studies indicate a strong correlation between cardiolipin content and increase in mitochondrial function with exercise [40; 73; 89; 90], but it has not been evaluated as a general mitochondrial biomarker in disease. With no single best mitochondrial marker, a good strategy is to quantify several different biomarkers to minimize the decorrelating effects caused by diseases, treatments, or other factors. Determination of multiple markers, particularly a matrix marker and a marker from the mtIM, allows tracking changes in mitochondrial quality defined by their ratio.

5. Normalization of rate per system

5.1. Flow: per chamber

The experimental system (chamber) is part of the measurement instrument, separated from the environment as a closed, open, isothermal or non-isothermal system (**Table 4**). Reporting O_2 flows per respiratory chamber, I_{O_2} [nmol·s^{-1}], restricts the analysis to intra-experimental comparison of relative differences.

5.2. Flux: per chamber volume

5.2.1. System-specific flux J_{V,O_2}: We distinguish between (*1*) the *system* with volume V and mass m defined by the system boundaries and its total contents, and (*2*) the *sample* of X with volume V_X and mass m_X enclosed in the experimental chamber

Table 6. Conversion of various formats and units used in respirometry and ergometry to SI units (International System of Units [11]). z_B is the charge number, which is the number of electrons e^- or reducing equivalents N_e per elementary entity U_B.

Format	1 Unit	·	Multiplication factor	SI-unit	Notes
$\underline{n}$	ng.atom $O \cdot s^{-1}$	$(z_O = 2)$	0.5	nmol $O_2 \cdot s^{-1}$	
$\underline{n}$	ng.atom $O \cdot min^{-1}$	$(z_O = 2)$	8.333	pmol $O_2 \cdot s^{-1}$	
$\underline{n}$	natom $O \cdot min^{-1}$	$(z_O = 2)$	8.333	pmol $O_2 \cdot s^{-1}$	
$\underline{n}$	nmol $O_2 \cdot min^{-1}$	$(z_{O_2} = 4)$	16.67	pmol $O_2 \cdot s^{-1}$	
$\underline{n}$	nmol $O_2 \cdot h^{-1}$	$(z_{O_2} = 4)$	0.2778	pmol $O_2 \cdot s^{-1}$	
$\underline{V}$ to $\underline{n}$	mL $O_2 \cdot min^{-1}$ at STPD		0.7443	µmol $O_2 \cdot s^{-1}$	1
$\underline{e}$ to $\underline{n}$	W = $J \cdot s^{-1}$ at -470 kJ·mol^{-1} O_2		-2.128	µmol $O_2 \cdot s^{-1}$	
$\underline{e}$ to $\underline{n}$	mA = mC·s^{-1}	$(z_{H^+} = 1)$	10.36	nmol $H^+ \cdot s^{-1}$	2
$\underline{e}$ to $\underline{n}$	mA = mC·s^{-1}	$(z_{O_2} = 4)$	2.591	nmol $O_2 \cdot s^{-1}$	2
$\underline{n}$ to $\underline{e}$	nmol $H^+ \cdot s^{-1}$	$(z_{H^+} = 1)$	0.09649	mA	3
$\underline{n}$ to $\underline{e}$	nmol $O_2 \cdot s^{-1}$	$(z_{O_2} = 4)$	0.3859	mA	3

1 At standard temperature and pressure dry (STPD: 0 °C = 273.15 K and 1 atm = 101.325 kPa = 760 mmHg), the molar volume of an ideal gas V_m is 22.414 and V_{m,O_2} is 22.392 L·mol^{-1}. Rounded to three decimal places, both values yield the conversion factor of 0.744. For comparison at normal temperature and pressure dry (NTPD: 20 °C), V_{m,O_2} is 24.038 L·mol^{-1}. Note that the SI standard pressure is 100 kPa.
2 The multiplication factor is $10^6/(z_B \cdot F)$.
3 The multiplication factor is $z_B \cdot F/10^6$.

(**Figure 5**). O_2 flow per object, $I_{O_2/X}$, is the total O_2 flow in the system divided by the number N_X of objects in the system. $I_{O_2/X}$ increases as the mass M_{UX} per object X is increased. Sample mass-specific O_2 flux, J_{O_2/m_S}, should be independent of the mass-concentration of the subsample obtained from the same tissue or cell culture, but system volume-specific O_2 flux J_{V,O_2} (per liquid volume of the experimental chamber) increases in proportion to the mass of the sample in the chamber. Although J_{V,O_2} depends on mass-concentration of the sample in the chamber, it should be independent of the chamber (system) volume at constant sample mass-concentration. There are practical limitations to increasing the mass-concentration of the sample in the chamber, when one is concerned about crowding effects and instrumental time resolution. The wall of the instrumental chamber and the enclosed solid stirrer are not counted as part of the experimental chamber volume.

5.2.2. Advancement per volume: When the reactor volume does not change during the reaction, which is typical for liquid phase reactions, the volume-specific *flux of a chemical reaction* r is the time derivative of the advancement of the reaction per unit volume, $J_{V,rB} = \mathrm{d}_r\xi_B/\mathrm{d}t \cdot V^{-1}$ [(mol·s^{-1})·L^{-1}]. The *rate of concentration change* is $\mathrm{d}c_B/\mathrm{d}t$ [(mol·L^{-1})·s^{-1}], where concentration is $c_B = n_B \cdot V^{-1}$. There is a difference between (*1*) J_{V,rO_2} [mol·s^{-1}·L^{-1}] and (*2*) rate of concentration change [mol·L^{-1}·s^{-1}]. These merge into a single expression only in closed systems. In open systems, internal transformations (catabolic flux, O_2 consumption) are distinguished from external flux (such as O_2 supply). External fluxes of all substances are zero in closed systems. In a closed chamber O_2 consumption (internal flow I_{kO_2} [pmol·s^{-1}] of catabolic reactions k) causes a decline in the amount n_{O_2} [nmol] of O_2 in the system. Normalization of these quantities for the volume V [L] of the system yields volume-specific O_2 flux, $J_{V,kO_2} = I_{kO_2} \cdot V^{-1}$ [nmol·s^{-1}·L^{-1}], and O_2 concentration, $[O_2]$ or $c_{O_2} = n_{O_2} \cdot V^{-1}$ [µmol·L^{-1} = µM = nmol·mL^{-1}]. Instrumental background O_2 flux is due to external flux into a non-ideal closed respirometer, so total volume-specific flux has to be corrected for instrumental background O_2 flux—O_2 diffusion into or out of the experimental chamber. $J_{V,\mathrm{kO_2}}$ is relevant mainly for methodological reasons and should be compared with the accuracy of instrumental resolution of background-corrected flux, *e.g.*, ±1 nmol·s^{-1}·L^{-1} [51]. 'Catabolic' indicates O_2 flux $J_{\mathrm{kO_2}}$ corrected for: (*1*) instrumental background O_2 flux; (*2*) chemical background O_2 flux due to autoxidation of chemical components added to the incubation medium; and (*3*) *Rox* of O_2-consuming side reactions unrelated to the catabolic pathway k.

6. Conversion of units

Many different units have been used to report the O_2 consumption rate OCR (**Table 6**). SI base units provide the common reference to introduce the theoretical principles (**Figure 5**), and are used with appropriately chosen SI prefixes to express numerical data in the most practical format, with an effort towards unification within specific areas of application (**Table 7**). Reporting data in SI units—including the mole [mol], coulomb [C], joule [J], and second [s]—should be encouraged, particularly by journals that propose the use of SI units.

Although volume is expressed as m^3 using the SI base unit, the liter [L = dm^3] is a conventional unit of volume for concentration and is used for most solution chemical kinetics. If one multiplies $I_{\mathrm{O_2}/X}$ by C_X, then the result will not only be the amount of O_2 [mol] consumed per time [s^{-1}] in one liter [L^{-1}], but also the change in O_2 concentration per second (for any volume of an ideally closed system). This is ideal for kinetic modeling as it blends with chemical rate equations where concentrations are typically expressed in mol·L^{-1} [136]. In studies of multinuclear cells—such as differentiated skeletal muscle cells—it is easy to determine the number of nuclei but not the total number of cells. A generalized concept, therefore, is obtained by substituting cells by nuclei as the elementary entity. This does not hold, however, for non-nucleated platelets.

For studies of cells, we recommend that respiration be expressed, as far as possible, as: (*1*) O_2 flux normalized for a mitochondrial marker, for separation of the effects of mitochondrial quality and content on cell respiration (this includes *FCR*s as a normalization for a functional mitochondrial marker); (*2*) O_2 flux in units of cell volume or mass, for comparison of respiration of cells with different cell size [113] and with studies on tissue preparations, and (*3*) O_2 flow in units of attomole (10^{-18} mol) of O_2 consumed per second by each individual cell [amol·s^{-1}·x^{-1}], numerically equivalent to [pmol·s^{-1}·(10^6 x)$^{-1}$]. This convention allows information to be easily used when designing experiments in which O_2 flow must be considered. For example, to estimate the volume-specific O_2 flux in an experimental chamber that would be expected at a particular cell-count concentration, one simply needs to multiply the flow per cell by the number of cells per volume of interest. This provides the amount of O_2 [mol] consumed per time [s^{-1}] per unit volume [L^{-1}]. At an O_2 flow of 100 amol·s^{-1}·x^{-1} and a cell-count concentration of 10^9 x·L^{-1} (= 10^6 x·mL^{-1}), the chamber volume-specific O_2 flux is 100 nmol·s^{-1}·L^{-1} (= 100 pmol·s^{-1}·mL^{-1}).

ET capacity in human cell types including HEK 293, primary HUVEC, and fibroblasts ranges from 50 to 180 amol·s^{-1}·x^{-1}, measured in living cells in the noncoupled state [54]. At 100 amol·s^{-1}·x^{-1} corrected for *Rox*, the current across the mt- membranes, I_{el}, approximates 193 pA·x^{-1} or 0.2 nA per cell. See Rich [115] for an extension of quantitative bioenergetics from the molecular to the human scale, with a transmembrane proton flux equivalent to 520 A in an adult at a catabolic power of -110 W·x^{-1}. Modelling approaches illustrate the link between protonmotive force and currents [143].

We consider isolated mitochondria as powerhouses and proton pumps as molecular machines to relate experimental results to energy metabolism of living cells. The cellular P»/O_2 based on oxidation of glycogen is increased by the glycolytic (fermentative) substrate-level phosphorylation of 3 P»/Glyc or 0.5 mol P» for each mol O_2 consumed in the complete oxidation of a mol glycosyl-unit (Glyc).

Table 7. Conversion of units with preservation of numerical values.

Name	Frequently used unit	Equivalent unit	Notes
volume-specific flux $J_{V,O2}$	pmol·s^{-1}·mL^{-1}	nmol·s^{-1}·L^{-1}	1
	mmol·s^{-1}·L^{-1}	mol·s^{-1}·m^{-3}	2
flow per cell $I_{O2/ce}$	pmol·s^{-1}·Mx^{-1}	amol·s^{-1}·x^{-1}	3
	pmol·s^{-1}·Gx^{-1}	zmol·s^{-1}·x^{-1}	4
cell-count concentration C_{ce}	10^6 x·mL^{-1}	10^9 x·L^{-1}	
mitochondrial protein concentration C_{mtE}	0.1 mg·mL^{-1}	0.1 g·L^{-1}	
sample mass-specific flux $J_{O2/mX}$	pmol·s^{-1}·mg^{-1}	nmol·s^{-1}·g^{-1}	5
catabolic power P_k	µW·Mx^{-1}	pW·x^{-1}	1, 3
volume V	1000 L	m^3 (1000 kg)	
	L	dm^3 (kg)	
	mL	cm^3 (g)	
	µL	mm^3 (mg)	
	fL	µm^3 (pg)	6
amount of substance concentration, n_B	M = mol·L^{-1}	mol·dm^{-3}	

1 pmol: picomole = 10^{-12} mol
2 mmol: millimole = 10^{-3} mol
3 amol: attomole = 10^{-18} mol; 1 Mx = 10^6 x
4 zmol: zeptomole = 10^{-21} mol; 1 Gx = 10^9 x
5 nmol: nanomole = 10^{-9} mol
6 fL: femtoliter = 10^{-15} L; µL: microliter = 10^{-6} L

Adding 0.5 to the mitochondrial P»/O_2 ratio of 5.4 yields a bioenergetic cell physiological P»/O_2 ratio close to 6. Two NADH equivalents are formed during glycolysis and transported from the cytosol into the mitochondrial matrix, either by the malate-aspartate shuttle or by the glycerophosphate shuttle (**Figure 1a**) resulting in different theoretical yields of ATP generated by mitochondria, the energetic cost of which potentially must be taken into account. Considering also substrate-level phosphorylation in the TCA cycle, this high P»/O_2 ratio not only reflects proton translocation and OXPHOS studied in isolation, but integrates mitochondrial physiology with energy transformation in the living cell [49].

7. Conclusions

Catabolic cell respiration is the process of exergonic and exothermic energy transformation in which scalar redox reactions are coupled to vectorial ion translocation across a semipermeable membrane, which separates the small volume of a bacterial cell or mitochondrion from the larger volume of its surroundings. The electrochemical exergy can be partially conserved in the phosphorylation of ADP to ATP or in ion pumping, or dissipated in an electrochemical short-circuit. Respiration is thus clearly distinguished from fermentation as the counterparts of cellular core energy metabolism. O_2 flux balance schemes illustrate the relationships and general definitions (**Overview, Figure 1**).

Experimentally, respiration is separated in mitochondrial preparations from the interactions with the fermentative pathways of the living cell. OXPHOS analysis is based on the study of mitochondrial preparations complementary to bioenergetic investigations of (*1*) submitochondrial particles and molecular structures, (*2*) living cells, and (*3*) organisms—from model organisms to the human species including healthy and diseased persons (patients).

Box 3: Recommendations for studies with mitochondrial preparations

- Normalization of respiratory rates should be provided as far as possible:

A. Sample normalization

1. *Object count-specific biophysical normalization*: O_2 flow on a per single cell

or per single organism basis; this may not be possible when dealing with coenocytic organisms, *e.g.*, filamentous fungi, or tissues without cross-walls separating individual cells, *e.g.*, muscle fibers.

2. *Size-specific cellular normalization*: per g protein; per organism-, cell- or tissue-mass as mass-specific O_2 flux; per cell volume as cell volume-specific flux.
3. *Mitochondrial normalization*: per mitochondrial marker as mt-specific flux.

B. Chamber normalization

1. Chamber volume-specific flux J_V [pmol·s^{-1}·mL^{-1}] is reported for quality control in relation to instrumental sensitivity and limit of detection of volume-specific flux.
2. Sample concentration in the experimental chamber is reported as count concentration, mass concentration, or mitochondrial concentration; this is a component of the measuring conditions. With information on cell size and the use of multiple normalizations, maximum potential information is available [54; 113; 136]. Reporting exclusively flow in a respiratory chamber [nmol·s^{-1}] is discouraged, since it restricts the analysis to intra-experimental comparison of relative (qualitative) differences.

- Catabolic mitochondrial respiration is distinguished from residual O_2 consumption. Fluxes in mitochondrial coupling states should be, as far as possible, corrected for residual O_2 consumption.

- Different mechanisms of uncoupling should be distinguished by defined terms. The tightness of coupling relates to these uncoupling mechanisms, whereas the coupling stoichiometry varies as a function the substrate type involved in ET pathways with either three or two redox proton pumps operating in series. Separation of tightness of coupling from the pathway-dependent coupling stoichiometry is possible only when the substrate type undergoing oxidation remains the same for respiration in LEAK-, OXPHOS-, and ET states. In studies of the tightness of coupling, therefore, simple substrate-inhibitor combinations should be applied to exlcude a shift in substrate competition that may occur when providing physiological substrate cocktails.

- In studies of isolated mitochondria, the mitochondrial recovery and yield should be reported. Experimental criteria such as transmission electron microscopy for evaluation of purity versus integrity should be considered. Mitochondrial markers—such as citrate synthase activity as an enzymatic matrix marker—provide a link to the tissue of origin on the basis of calculating the mitochondrial recovery, *i.e.*, the fraction of mitochondrial marker obtained from a unit mass of tissue. Total mitochondrial protein is frequently applied as a mitochondrial marker, which is restricted to isolated mitochondria.

- In studies of permeabilized cells, the viability of the cell culture or cell suspension of origin should be reported. Normalization should be evaluated for total cell count or viable cell count.

- Terms and symbols are summarized in **Table 8**. Their use will facilitate transdisciplinary communication and support further development of a consistent theory of bioenergetics and mitochondrial physiology. Technical terms related to and defined with practical words can be used as index terms in data repositories, support the creation of ontologies towards semantic information processing (MitoPedia), and help in communicating analytical findings as impactful data-driven stories. '*Making data available without making it understandable may be worse than not making it available at all*' [99]. Success will depend on taking further steps: (*1*) exhaustive text-mining considering Omics data and functional data; (*2*) network analysis of Omics data with bioinformatics tools; (*3*) cross-validation with distinct bioinformatics approaches; (*4*) correlation with physiological data; (*5*) guidelines for biological validation of network data. This is a call to carefully contribute to FAIR principles (Findable, Accessible, Interoperable, Reusable) for the sharing of scientific data.

Table 8. Terms, symbols, and units. SI base units are used, except for the liter [L = dm³]. SI refers to ref. [11], IUPAC refers to ref. [24].

Term	Symbol	Unit	Links and comments
adenosine diphosphate	ADP		Tab. 1; Fig. 1, 2, 5
adenosine monophosphate	AMP		2 ADP ↔ ATP+AMP
adenosine triphosphate	ATP		Fig. 2, 5
adenylates	AMP, ADP, ATP		Section 2.5.1
alternative quinol oxidase	AOX		Fig. 1B
amount of substance B	n_B or n(B)	[mol]	IUPAC
ATP yield per O_2	$Y_{P»/O2}$	1	$Y_{P»/O2} = J_{P»}/J_{kO2}$; P»/$O_2$ measured in any respiratory state
catabolic rate of respiration	J_{kO2}; I_{kO2}	*varies*	Fig. 1, 3; *see* flux J and flow I
catabolic reaction	k		Fig. 1, 3
cell count	N_{ce}	[x]	Tab. 4; Fig. 5; *see* number of cells
cell-count concentration	C_{ce}	[x·L⁻¹]	Tab. 4; $C_{ce} = N_{ce} \cdot V^{-1}$
cell mass	m_{ce}	[kg]	Tab. 5; Fig. 5
cell mass, mass per cell	M_{Uce}	[kg·x⁻¹]	Tab. 5; Fig. 5
cell-mass concentration	C_{mce}	[kg·L⁻¹]	$C_{mce} = m_{ce} \cdot V^{-1}$; Tab. 4; *see* C_{mX}
cell viability index	VI_{ce}		$VI_{ce} = N_{vce} \cdot N_{ce}^{-1} = 1 - N_{dce} \cdot N_{ce}^{-1}$
charge number per U_B	z_B	1	Tab. 6; $z_{O2} = 4$; ($z_B = Q_B \cdot e^{-1}$ [24])
Complexes I to IV	CI to CIV		respiratory Complexes CI to CVI are redox proton pumps of the ETS, but not F_1F_O-ATPase; hence the term CV is not recommended; Fig. 1B
concentration of B, amount	$c_B = n_B \cdot V^{-1}$	[mol·L⁻¹]	SI: amount of substance concentration (IUPAC)
concentration of O_2, amount	$c_{O2} = n_{O2} \cdot V^{-1}$	[mol·L⁻¹]	[O_2]; Box 2
concentration of X, count	$C_X = N_X \cdot V^{-1}$	[x·L⁻¹]	Tab. 4 (IUPAC: number concentration)
count format	$\underline{N}$	[x]	Tab. 4, 5; Fig. 5
count of entity-type X	N_X	[x]	SI; *see* number of entities X
coupling-control state	CCS		Section 2.4.1
dead cells	dce		Tab. 5
electrical format	$\underline{e}$	[C]	Tab. 6
electron transfer, state	ET		Tab. 1; Fig. 2B, 4 (State 3u)
electron transfer system	ETS		Fig. 2B, 4 (electron transport chain)
elementary entity of entity-type X	U_X	[x]	single countable object; Tab. 4, 5
ET capacity	E	*varies*	rate; Tab. 1; Fig. 2
ET-excess capacity	E-P	*varies*	Fig. 2
flow, for O_2	I_{O2}	[mol·s⁻¹]	system-related or count-specific extensive quantity; Fig. 5
flux, for O_2	J_{O2}	*varies*	size-specific quantity; Fig. 5
flux control ratio	*FCR*	1	background/reference flux; Fig.5
inorganic phosphate	P_i		Fig. 1C
inorganic phosphate carrier	PiC		Fig. 1C
isolated mitochondria	imt		Tab. 5
LEAK respiration	L	*varies*	rate; Tab. 1; Fig. 2
LEAK state	LEAK		Tab. 1; Fig. 2 (compare State 4)
living cells, entity-type	ce		Tab. 5 (intact cells)
mass, dry mass	m_d	[kg]	Fig. 5 (dry weight) [56]

mass, wet mass	m_w	[kg]	Fig. 5 (wet weight)
mass concentration in a mixture	C_{mX}	[kg·L^{-1}]	Tab. 4
mass format	<u>m</u>	[kg]	Tab. 4
mass of sample of X in a mixture	m_X	[kg]	SI: mass m_S of pure sample S
mass per elementary entity U_X, mass per individual object	M_{UX}	[kg·x^{-1}]	body mass; Fig. 5; Tab. 4; SI: $m(X)$ (*compare* molar mass M_B [kg·mol^{-1}])
MITOCARTA			https://www.broadinstitute.org/scientific-community/science/programs/metabolic-disease-program/publications/mitocarta/mitocarta-in-0 [13]
mitochondria or mitochondrial	mt		Box 1
mitochondrial concentration	$C_{mtE} = mtE·V^{-1}$	[*mt*EU·L^{-1}]	per chamber volume; Tab. 4
mitochondrial content per U_X	mtE_{UX}	[*mt*EU·x^{-1}]	$mtE_{UX} = mtE·N_X^{-1}$; Tab. 4
mitochondrial density per m_X	$D_{mtE/mX}$	[*mt*EU·kg^{-1}]	$D_{mtE/mX} = mtE·m_X^{-1}$; Tab. 4
mitochondrial density per V_X	$D_{mtE/VX}$	[*mt*EU·L^{-1}]	$D_{mtE/VX} = mtE·V_X^{-1}$; Tab. 4
mitochondrial DNA	mtDNA		Box 1
mitochondrial elementary marker	*mtE*	[*mt*EU]	quantity of mt-marker; Tab. 4
mitochondrial elementary unit	*mt*EU	*varies*	specific units for mt-marker; Tab. 4
mitochondrial inner membrane	mtIM		Fig. 1; Box 1 (MIM)
mitochondrial outer membrane	mtOM		Fig. 1; Box 1 (MOM)
mitochondrial recovery	Y_{mtE}	1	fraction of *mtE* recovered from the tissue sample in imt-stock
mitochondrial yield	$Y_{mtE/mX}$	[*mt*EU·kg^{-1}]	mt-yield in imt-stock per mass of tissue sample; $Y_{mtE/mX}=Y_{mtE}·D_{mtE}$
MitoPedia		http://www.bioblast.at/index.php/MitoPedia	
molar format	<u>n</u>	[mol]	Tab. 6
molar mass	M_B	[kg·mol^{-1}]	*compare* M_{UB} [kg·x^{-1}]; SI $M(X)$
negative	neg		Fig. 4
number of cells	N_{ce}	[x]	total cell count of living cells, $N_{ce} = N_{vce} + N_{dce}$; Tab. 4, 5
number of dead cells	N_{dce}	[x]	non-viable cell count, loss of plasma membrane barrier function; Tab. 5
number of entities B, count	$N_B = N·U_B$	[x]	Tab. 4 (IUPAC)
number of elementary entities, count of X	$N_X = N·U_X$	[x]	'count' is an SI quantity [11], but the elementary unit [x] is not in the SI [95]; Tab. 4; Fig. 5
number of viable cells, count	N_{vce}	[x]	viable cell count, intact plasma membrane barrier function; Tab. 5
organisms, entity-type	org		Tab. 5
oxidative phosphorylation	OXPHOS		Tab. 1
OXPHOS capacity	*P*	*varies*	rate; Tab. 1; Fig. 2
OXPHOS state	OXPHOS		Tab. 1; Fig. 2; OXPHOS state distinguished from the process OXPHOS (State 3 at kinetically-saturating [ADP] and [P$_i$])
oxygen concentration	$c_{O_2} = n_{O_2}·V^{-1}$	[mol·L^{-1}]	[O$_2$]; Section 3.2
oxygen flux, in reaction r	J_{rO_2}	*varies*	Overview
pathway-control state	PCS		Section 2.2

permeability transition	mtPT		Fig. 3; Section 2.4.3 (MPT)
permeabilized cells, entity-type	pce		experimental permeabilization of plasma membrane; Tab. 5
permeabilized muscle fibers	pfi		Tab. 5
permeabilized tissue	pti		Tab. 5
phosphorylation of ADP to ATP	P»		Tab. 1, 2; Fig. 1, 4
P»/O_2 ratio	P»/O_2	1	mechanistic $Y_{P»/O_2}$, calculated from pump stoichiometries; Fig. 1c
positive	pos		Fig. 4
proton in the neg compartment	H^+_{neg}	[x]	Fig. 4
proton in the pos compartment	H^+_{pos}	[x]	Fig. 4
protonmotive force	*pmF*	[V]	Overview; Tab. 1; Fig 1a, 2, 4
rate in ET state	*E*	*varies*	ET capacity; Tab. 1; Fig. 2, 4
rate in LEAK state	*L*	*varies*	Tab. 1: *L*(n), *L*(T), *L*(Omy); Fig. 2
rate in OXPHOS state	*P*	*varies*	OXPHOS capacity; Tab.1; Fig. 2, 4
rate in ROX state	*Rox*	*varies*	Overview; Tab. 1
residual oxygen consumption	ROX; *Rox*		state ROX; rate *Rox*; Tab. 1
respiration	J_{rO_2}	*varies*	rate of reaction r; Overview
respiratory supercomplex	$SCI_nIII_nIV_n$		supramolecular assemblies with variable copy numbers (*n*) of CI, CIII and CIV; Box 1
sample of *X* in a mixture	s		$V_X < V$; Tab. 4, 5
substrate concentration at half-maximal rate	c_{50}	[mol·L^{-1}]	Section 2.1.2
substrate-uncoupler-inhibitor-titration	SUIT		Section 2.2
tissue homogenate	thom		Tab. 5
viable cells	vce		Tab. 5
volume format	$\underline{V}$	[L]	Tab. 6
volume of experimental chamber	*V*	[L]	*V* with s; Tab. 4, 7; Fig. 5
volume of sample of *X* in a mixture	V_X	[L]	Fig. 5; Tab. 5

Different mechanisms of respiratory uncoupling have to be distinguished (**Figure 3**). Metabolic fluxes measured in defined coupling- and pathway-control states (**Figures 1, 2 and 4**) provide insights into the meaning of cellular and organismic respiration.

The optimal choice for expressing mitochondrial and cell respiration as O_2 flow per biological sample, and normalization for specific tissue-markers (volume, mass, protein) and mitochondrial markers (volume, protein, content, mtDNA, activity of marker enzymes, respiratory reference state) is guided by the scientific question under study. Interpretation of the data depends critically on appropriate normalization (**Figure 5**).

Results are comparable between studies only, if respirometric measurements are normalized for defined quantities of sample. For some samples it is informative, if quantification is possible in terms of a count (number of countable objects). Using cells as an example, a distinction is made between sample type (cells) and the quantity of cells (count, mass, volume). Using the unit [mol·s^{-1}·cell^{-1}] has been common but is ambiguous. This is resolved by (*1*) not only indicating the *entity-type* (cell), but (*2*) additionally defining the *quantity* (count [x], mass [kg], volume [L]) in which the entity is expressed with corresponding units. Similarly, substance concentrations can be expressed in various formats with corresponding units, including molecular count concentration, $C_{O_2} = N_{O_2}·V^{-1}$ [x·L^{-1}], and molar amount concentration, $c_{O_2} = n_{O_2}·V^{-1}$ [mol·L^{-1}], whereas it does not make sense to write [O_2·L^{-1}]. In conclusion, expressions such as [cells·L^{-1}] or [mol·s^{-1}·cell^{-1}] should be replaced by [x·L^{-1}] or [mol·s^{-1}·x^{-1}]. Symbols for quantities, such as C_X for count concentration, gain meaning only in context with specification of the entity-type, *e.g.*, cell types, growth conditions. Simple symbols can be used, *e.g.*, M for body mass [kg·x^{-1}], if clarity of definition is provided in the text.

MitoEAGLE can serve as a gateway to better diagnose mitochondrial respiratory adaptations and defects linked to genetic variation, age-related health risks, sex-specific mitochondrial performance, lifestyle with its effects on degenerative diseases, and thermal and chemical environment. The present recommendations on coupling-control states and rates are focused on studies using mitochondrial preparations (**Box 3**). These will be extended in a series of reports on pathway control of mitochondrial respiration, respiratory states and rates in living cells, respiratory flux control ratios, and harmonization of experimental procedures.

References

1. Altmann R (1894) Die Elementarorganismen und ihre Beziehungen zu den Zellen. Zweite vermehrte Auflage. Verlag Von Veit & Comp, Leipzig:160 pp.
2. Baggeto LG, Testa-Perussini R (1990) Role of acetoin on the regulation of intermediate metabolism of Ehrlich ascites tumor mitochondria: its contribution to membrane cholesterol enrichment modifying passive proton permeability. Arch Biochem Biophys 283:341-8.
3. Beard DA (2005) A biophysical model of the mitochondrial respiratory system and oxidative phosphorylation. PLoS Comput Biol 1(4):e36.
4. Benda C (1898) Weitere Mitteilungen über die Mitochondria. Verh Dtsch Physiol Ges:376-83.
5. Birkedal R, Laasmaa M, Vendelin M (2014) The location of energetic compartments affects energetic communication in cardiomyocytes. Front Physiol 5:376.
6. Blier PU, Dufresne F, Burton RS (2001) Natural selection and the evolution of mtDNA-encoded peptides: evidence for intergenomic co-adaptation. Trends Genet 17:400-6.
7. Blier PU, Guderley HE (1993) Mitochondrial activity in rainbow trout red muscle: the effect of temperature on the ADP-dependence of ATP synthesis. J Exp Biol 176:145-58.
8. Boushel RC, Gnaiger E, Schjerling P, et al (2007) Patients with Type 2 diabetes have normal mitochondrial function in skeletal muscle. Diabetologia 50:790-6.
9. Breton S, Beaupré HD, Stewart DT, et al (2007) The unusual system of doubly uniparental inheritance of mtDNA: isn't one enough? Trends Genet 23:465-74.
10. Brown GC (1992) Control of respiration and ATP synthesis in mammalian mitochondria and cells. Biochem J 284:1-13.
11. Bureau International des Poids et Mesures (2019) The International System of Units (SI). 9th edition:117-216 ISBN 978-92-822-2272-0.
12. Burger G, Gray MW, Forget L, Lang BF (2013) Strikingly bacteria-like and gene-rich mitochondrial genomes throughout jakobid protists. Genome Biol Evol 5:418-38.
13. Calvo SE, Klauser CR, Mootha VK (2016) MitoCarta2.0: an updated inventory of mammalian mitochondrial proteins. Nucleic Acids Research 44:D1251-7.
14. Calvo SE, Julien O, Clauser KR, et al (2017) Comparative analysis of mitochondrial N-termini from mouse, human, and yeast. Mol Cell Proteomics 16:512-23.
15. Campos JC, Queliconi BB, Bozi LHM, et al (2017) Exercise reestablishes autophagic flux and mitochondrial quality control in heart failure. Autophagy 13:1304-317.
16. Canton M, Luvisetto S, Schmehl I, Azzone GF (1995) The nature of mitochondrial respiration and discrimination between membrane and pump properties. Biochem J 310:477-81.
17. Carrico C, Meyer JG, He W, et al (2018) The mitochondrial acylome emerges: proteomics, regulation by Sirtuins, and metabolic and disease implications. Cell Metab 27:497-512.
18. Chan DC (2006) Mitochondria: dynamic organelles in disease, aging, and development. Cell 125:1241-52.
19. Chance B, Williams GR (1955a) Respiratory enzymes in oxidative phosphorylation. I. Kinetics of oxygen utilization. J Biol Chem 217:383-93.
20. Chance B, Williams GR (1955b) Respiratory enzymes in oxidative phosphorylation: III. The steady state. J Biol Chem 217:409-27.
21. Chance B, Williams GR (1956) The respiratory chain and oxidative phosphorylation. Adv Enzymol Relat Subj Biochem 17:65-134.
22. Chowdhury SK, Djordjevic J, Albensi B, Fernyhough P (2015) Simultaneous

evaluation of substrate-dependent oxygen consumption rates and mitochondrial membrane potential by TMRM and safranin in cortical mitochondria. Biosci Rep 36:e00286.
23. Cobb LJ, Lee C, Xiao J, et al (2016) Naturally occurring mitochondrial-derived peptides are age-dependent regulators of apoptosis, insulin sensitivity, and inflammatory markers. Aging (Albany NY) 8:796-809.
24. Cohen ER, Cvitas T, Frey JG, et al (2008) Quantities, units and smbols in physical chemistry, IUPAC Green Book, 3rd Edition, 2nd Printing, IUPAC & RSC Publishing, Cambridge.
25. Cooper H, Hedges LV, Valentine JC, eds (2009) The handbook of research synthesis and meta-analysis. Russell Sage Foundation.
26. Coopersmith J (2010) Energy, the subtle concept. The discovery of Feynman's blocks from Leibnitz to Einstein. Oxford University Press:400 pp.
27. Cummins J (1998) Mitochondrial DNA in mammalian reproduction. Rev Reprod 3:172-82.
28. Dai Q, Shah AA, Garde RV, et al (2013) A truncated progesterone receptor (PR-M) localizes to the mitochondrion and controls cellular respiration. Mol Endocrinol 27:741-53.
29. Daum B, Walter A, Horst A, et al (2013) Age-dependent dissociation of ATP synthase dimers and loss of inner-membrane cristae in mitochondria. Proc Natl Acad Sci U S A 110:15301-6.
30. Diebold LP, Gil HJ, Gao P, et al (2019) Mitochondrial Complex III is necessary for endothelial cell proliferation during angiogenesis. Nat Metab 1:158–71.
31. Divakaruni AS, Brand MD (2011) The regulation and physiology of mitochondrial proton leak. Physiology (Bethesda) 26:192-205.
32. Doerrier C, Garcia-Souza LF, Krumschnabel G, et al (2018) High-Resolution FluoRespirometry and OXPHOS protocols for human cells, permeabilized fibres from small biopsies of muscle, and isolated mitochondria. Methods Mol Biol 1782:31-70.
33. Doskey CM, van 't Erve TJ, Wagner BA, Buettner GR (2015) Moles of a substance per cell is a highly informative dosing metric in cell culture. PLoS One 10:e0132572.
34. Drahota Z, Milerová M, Stieglerová A, et al (2004) Developmental changes of cytochrome *c* oxidase and citrate synthase in rat heart homogenate. Physiol Res 53:119-22.
35. Duarte FV, Palmeira CM, Rolo AP (2014) The role of microRNAs in mitochondria: small players acting wide. Genes (Basel) 5:865-86.
36. Ehinger JK, Morota S, Hansson MJ, et al (2015) Mitochondrial dysfunction in blood cells from amyotrophic lateral sclerosis patients. J Neurol 262:1493-503.
37. Ehinger JK, Piel S, Ford R, et al (2016) Cell-permeable succinate prodrugs bypass mitochondrial complex I deficiency. Nat Commun 7:12317.
38. Ernster L, Schatz G (1981) Mitochondria: a historical review. J Cell Biol 91:227s-55s.
39. Estabrook RW (1967) Mitochondrial respiratory control and the polarographic measurement of ADP:O ratios. Methods Enzymol 10:41-7.
40. Faber C, Zhu ZJ, Castellino S, et al (2014) Cardiolipin profiles as a potential biomarker of mitochondrial health in diet-induced obese mice subjected to exercise, diet-restriction and ephedrine treatment. J Appl Toxicol 34:1122-9.
41. Falk MJ, ed (2020) Mitochondrial disease genes compendium. 1st ed. Academic Press:548 pp.
42. Feagin JE, Harrell MI, Lee JC, et al (2012) The fragmented mitochondrial ribosomal RNAs of *Plasmodium falciparum*. PLoS One 7:e38320.
43. Fell D (1997) Understanding the control of metabolism. Portland Press.
44. Forstner H, Gnaiger E (1983) Calculation of equilibrium oxygen concentration. In: Polarographic Oxygen Sensors. Aquatic and Physiological Applications. Gnaiger E, Forstner H (eds), Springer, Berlin, Heidelberg, New York:321-33.
45. Garlid KD, Beavis AD, Ratkje SK (1989) On the nature of ion leaks in energy-transducing membranes. Biochim Biophys Acta 976:109-20.
46. Garlid KD, Semrad C, Zinchenko V (1993) Does redox slip contribute significantly to mitochondrial respiration? In: Schuster S, Rigoulet M, Ouhabi R, Mazat J-P, eds. Modern trends in biothermokinetics. Plenum Press, New York, London:287-93.
47. Gebert N, Joshi AS, Kutik S, et al (2009) Mitochondrial cardiolipin involved in outer-membrane protein biogenesis: implications for Barth syndrome. Curr Biol 19:2133-9.
48. Gerö D, Szabo C (2016) Glucocorticoids suppress mitochondrial oxidant production via upregulation of uncoupling protein 2 in hyperglycemic endothelial cells. PLoS One 11:e0154813.
49. Gnaiger E (1993a). Efficiency and power strategies under hypoxia. Is low efficiency at high glycolytic ATP production a paradox?

In: Surviving Hypoxia: Mechanisms of Control and Adaptation. Hochachka PW, Lutz PL, Sick T, et al, eds. CRC Press, Boca Raton, Ann Arbor, London, Tokyo:77-109.
50. Gnaiger E (1993b) Nonequilibrium thermodynamics of energy transformations. Pure Appl Chem 65:1983-2002.
51. Gnaiger E (2001) Bioenergetics at low oxygen: dependence of respiration and phosphorylation on oxygen and adenosine diphosphate supply. Respir Physiol 128:277-97.
52. Gnaiger E (2008) Polarographic oxygen sensors, the oxygraph and high-resolution respirometry to assess mitochondrial function. In: Mitochondrial Dysfunction in Drug-Induced Toxicity (Dykens JA, Will Y, eds) John Wiley & Sons, Inc, Hoboken, NJ:327-52.
53. Gnaiger E (2009) Capacity of oxidative phosphorylation in human skeletal muscle. New perspectives of mitochondrial physiology. Int J Biochem Cell Biol 41:1837-45.
54. Gnaiger E (2020) Mitochondrial pathways and respiratory control. An introduction to OXPHOS analysis. 5th ed. Bioenerg Commun 2020.2.
55. Gnaiger E, Aasander Frostner E, Abdul Karim N, et al (2020) Mitochondrial respiratory states and rates. Nat Metab (in review)
56. Gnaiger E, Bitterlich G (1984) Proximate biochemical proposition and caloric content calculated from elemental CHN analysis: a stoichiometric concept. Oecologia 62:289-98.
57. Gnaiger E, Méndez G, Hand SC (2000) High phosphorylation efficiency and depression of uncoupled respiration in mitochondria under hypoxia. Proc Natl Acad Sci USA 97:11080-5.
58. Greggio C, Jha P, Kulkarni SS, et al (2017) Enhanced respiratory chain supercomplex formation in response to exercise in human skeletal muscle. Cell Metab 25:301-11.
59. Hinkle PC (2005) P/O ratios of mitochondrial oxidative phosphorylation. Biochim Biophys Acta 1706:1-11.
60. Hofstadter DR (1979) Gödel, Escher, Bach: An eternal golden braid. A metaphorical fugue on minds and machines in the spirit of Lewis Carroll. Harvester Press:499 pp.
61. Illaste A, Laasmaa M, Peterson P, Vendelin M (2012) Analysis of molecular movement reveals latticelike obstructions to diffusion in heart muscle cells. Biophys J 102:739-48.
62. Jasienski M, Bazzaz FA (1999) The fallacy of ratios and the testability of models in biology. Oikos 84:321-26.
63. Jepihhina N, Beraud N, Sepp M, et al (2011) Permeabilized rat cardiomyocyte response demonstrates intracellular origin of diffusion obstacles. Biophys J 101:2112-21.
64. Jezek P, Holendova B, Garlid KD, Jaburek M (2018) Mitochondrial uncoupling proteins: subtle regulators of cellular redox signaling. Antioxid Redox Signal 29:667-714.
65. Karnkowska A, Vacek V, Zubáčová Z, et al (2016) A eukaryote without a mitochondrial organelle. Curr Biol 26:1274-84.
66. Kenwood BM, Weaver JL, Bajwa A, et al (2013) Identification of a novel mitochondrial uncoupler that does not depolarize the plasma membrane. Mol Metab 3:114-23.
67. Klepinin A, Ounpuu L, Guzun R, et al (2016) Simple oxygraphic analysis for the presence of adenylate kinase 1 and 2 in normal and tumor cells. J Bioenerg Biomembr 48:531-48.
68. Koit A, Shevchuk I, Ounpuu L, et al (2017) Mitochondrial respiration in human colorectal and breast cancer clinical material is regulated differently. Oxid Med Cell Longev 1372640.
69. Komlódi T, Tretter L (2017) Methylene blue stimulates substrate-level phosphorylation catalysed by succinyl-CoA ligase in the citric acid cycle. Neuropharmacology 123:287-98.
70. Korn E (1969) Cell membranes: structure and synthesis. Annu Rev Biochem 38:263–88.
71. Lai N, M Kummitha C, Rosca MG, et al (2018) Isolation of mitochondrial subpopulations from skeletal muscle: optimizing recovery and preserving integrity. Acta Physiol (Oxf):e13182. doi: 10.1111/apha.13182.
72. Lane N (2005) Power, sex, suicide: mitochondria and the meaning of life. Oxford University Press:354 pp.
73. Larsen S, Nielsen J, Neigaard Nielsen C, et al (2012) Biomarkers of mitochondrial content in skeletal muscle of healthy young human subjects. J Physiol 590:3349-60.
74. Lee C, Zeng J, Drew BG, et al (2015) The mitochondrial-derived peptide MOTS-c promotes metabolic homeostasis and reduces obesity and insulin resistance. Cell Metab 21:443-54.
75. Lee SR, Kim HK, Song IS, et al (2013) Glucocorticoids and their receptors: insights into specific roles in mitochondria. Prog Biophys Mol Biol 112:44-54.
76. Leek BT, Mudaliar SR, Henry R, et al (2001) Effect of acute exercise on citrate synthase activity in untrained and trained human skeletal muscle. Am J Physiol Regul Integr Comp Physiol 280:R441-7.

77. Lemasters JJ, Nieminen AL, Qian T, et al (1998) The mitochondrial permeability transition in cell death: a common mechanism in necrosis, apoptosis and autophagy. Biochim Biophys Acta 1366:177-96.
78. Lemieux H, Blier PU, Gnaiger E (2017) Remodeling pathway control of mitochondrial respiratory capacity by temperature in mouse heart: electron flow through the Q-junction in permeabilized fibers. Sci Rep 7:2840.
79. Lemieux H, Semsroth S, Antretter H, et al (2011) Mitochondrial respiratory control and early defects of oxidative phosphorylation in the failing human heart. Int J Biochem Cell Biol 43:1729–38.
80. Lenaz G, Tioli G, Falasca AI, Genova ML (2017) Respiratory supercomplexes in mitochondria. In: Mechanisms of primary energy trasduction in biology. M Wikstrom (ed) Royal Society of Chemistry Publishing, London, UK:296-337.
81. Ling C, Rönn T (2019) Epigenetics in human obesity and type 2 diabetes. Cell Metab 29:1028-44. https://doi.org/10.1016/j.cmet.2019.03.009.
82. Lisowski P, Kannan P, Mlody B, Prigione A (2018) Mitochondria and the dynamic control of stem cell homeostasis. EMBO Rep 19:e45432.
83. Liu S, Roellig DM, Guo Y, et al (2016) Evolution of mitosome metabolism and invasion-related proteins in *Cryptosporidium*. BMC Genomics 17:1006.
84. Luo S, Valencia CA, Zhang J, et al (2018) Biparental inheritance of mitochondrial DNA in humans. Proc Natl Acad Sci U S A doi: 10.1073/pnas.1810946115.
85. Margulis L (1970) Origin of eukaryotic cells. New Haven: Yale University Press.
86. McDonald AE, Vanlerberghe GC, Staples JF (2009) Alternative oxidase in animals: unique characteristics and taxonomic distribution. J Exp Biol 212:2627-34.
87. McKenzie M, Lazarou M, Thorburn DR, Ryan MT (2006) Mitochondrial respiratory chain supercomplexes are destabilized in Barth Syndrome patients. J Mol Biol 361:462-9.
88. Menshikova EV, Ritov VB, Fairfull L, et al (2006) Effects of exercise on mitochondrial content and function in aging human skeletal muscle. J Gerontol A Biol Sci Med Sci 61:534-40.
89. Menshikova EV, Ritov VB, Ferrell RE, et al (2007) Characteristics of skeletal muscle mitochondrial biogenesis induced by moderate-intensity exercise and weight loss in obesity. J Appl Physiol (1985) 103:21-7.
90. Menshikova EV, Ritov VB, Toledo FG, et al (2005) Effects of weight loss and physical activity on skeletal muscle mitochondrial function in obesity. Am J Physiol Endocrinol Metab 288:E818-25.
91. Miller GA (1991) The science of words. Scientific American Library New York:276 pp.
92. Mitchell P (1961) Coupling of phosphorylation to electron and hydrogen transfer by a chemi-osmotic type of mechanism. Nature 191:144-8.
93. Mitchell P (2011) Chemiosmotic coupling in oxidative and photosynthetic phosphorylation. Biochim Biophys Acta Bioenergetics 1807:1507-38.
94. Mogensen M, Sahlin K, Fernström M, et al (2007) Mitochondrial respiration is decreased in skeletal muscle of patients with type 2 diabetes. Diabetes 56:1592-9.
95. Mohr PJ, Phillips WD (2015) Dimensionless units in the SI. Metrologia 52:40-7.
96. Moreno M, Giacco A, Di Munno C, Goglia F (2017) Direct and rapid effects of 3,5-diiodo-L-thyronine (T2). Mol Cell Endocrinol 7207:30092-8.
97. Morrow RM, Picard M, Derbeneva O, et al (2017) Mitochondrial energy deficiency leads to hyperproliferation of skeletal muscle mitochondria and enhanced insulin sensitivity. Proc Natl Acad Sci U S A 114:2705-10.
98. Murley A, Nunnari J (2016) The emerging network of mitochondria-organelle contacts. Mol Cell 61:648-53.
99. National Academies of Sciences, Engineering, and Medicine (2018) International coordination for science data infrastructure: Proceedings of a workshop—in brief. Washington, DC: The National Academies Press. doi: https://doi.org/10.17226/25015.
100. Oborník M (2019) In the beginning was the word: How terminology drives our understanding of endosymbiotic organelles. Microb Cell 6:134-41.
101. Oemer G, Lackner L, Muigg K, et al (2018) The molecular structural diversity of mitochondrial cardiolipins. Proc Nat Acad Sci U S A 115:4158-63.
102. Palmfeldt J, Bross P (2017) Proteomics of human mitochondria. Mitochondrion 33:2-14.
103. Paradies G, Paradies V, De Benedictis V, et al (2014) Functional role of cardiolipin in mitochondrial bioenergetics. Biochim Biophys Acta 1837:408-17.
104. Pesta D, Gnaiger E (2012) High-Resolution Respirometry. OXPHOS protocols for human cells and permeabilized fibres from small

biopsies of human muscle. Methods Mol Biol 810:25-58.
105. Pesta D, Hoppel F, Macek C, et al (2011) Similar qualitative and quantitative changes of mitochondrial respiration following strength and endurance training in normoxia and hypoxia in sedentary humans. Am J Physiol Regul Integr Comp Physiol 301:R1078–87.
106. Price TM, Dai Q (2015) The role of a mitochondrial progesterone receptor (PR-M) in progesterone action. Semin Reprod Med 33:185-94.
107. Puchowicz MA, Varnes ME, Cohen BH, et al (2004) Oxidative phosphorylation analysis: assessing the integrated functional activity of human skeletal muscle mitochondria – case studies. Mitochondrion 4:377-85.
108. Puntschart A, Claassen H, Jostarndt K, et al (1995) mRNAs of enzymes involved in energy metabolism and mtDNA are increased in endurance-trained athletes. Am J Physiol 269:C619-25.
109. Quiros PM, Mottis A, Auwerx J (2016) Mitonuclear communication in homeostasis and stress. Nat Rev Mol Cell Biol 17:213-26.
110. Rackham O, Mercer TR, Filipovska A (2012) The human mitochondrial transcriptome and the RNA-binding proteins that regulate its expression. WIREs RNA 3:675–95.
111. Rackham O, Shearwood AM, Mercer TR, et al (2011) Long noncoding RNAs are generated from the mitochondrial genome and regulated by nuclear-encoded proteins. RNA 17:2085-93.
112. Reichmann H, Hoppeler H, Mathieu-Costello O, et al (1985) Biochemical and ultrastructural changes of skeletal muscle mitochondria after chronic electrical stimulation in rabbits. Pflugers Arch 404:1-9.
113. Renner K, Amberger A, Konwalinka G, Gnaiger E (2003) Changes of mitochondrial respiration, mitochondrial content and cell size after induction of apoptosis in leukemia cells. Biochim Biophys Acta 1642:115-23.
114. Rice DW, Alverson AJ, Richardson AO, et al (2016) Horizontal transfer of entire genomes via mitochondrial fusion in the angiosperm *Amborella*. Science 342:1468-73.
115. Rich P (2003) Chemiosmotic coupling: The cost of living. Nature 421:583.
116. Rich PR (2013) Chemiosmotic theory. Encyclopedia Biol Chem 1:467-72.
117. Roger JA, Munoz-Gomes SA, Kamikawa R (2017) The origin and diversification of mitochondria. Curr Biol 27:R1177-92.
118. Rostovtseva TK, Sheldon KL, Hassanzadeh E, Monge C, et al (2008) Tubulin binding blocks mitochondrial voltage-dependent anion channel and regulates respiration. Proc Natl Acad Sci USA 105:18746-51.
119. Rustin P, Parfait B, Chretien D, et al (1996) Fluxes of nicotinamide adenine dinucleotides through mitochondrial membranes in human cultured cells. J Biol Chem 271:14785-90.
120. Saks VA, Veksler VI, Kuznetsov AV, et al (1998) Permeabilised cell and skinned fiber techniques in studies of mitochondrial function in vivo. Mol Cell Biochem 184:81-100.
121. Salabei JK, Gibb AA, Hill BG (2014) Comprehensive measurement of respiratory activity in permeabilized cells using extracellular flux analysis. Nat Protoc 9:421-38.
122. Sazanov LA (2015) A giant molecular proton pump: structure and mechanism of respiratory complex I. Nat Rev Mol Cell Biol 16:375-88.
123. Schneider TD (2006) Claude Shannon: biologist. The founder of information theory used biology to formulate the channel capacity. IEEE Eng Med Biol Mag 25:30-3.
124. Schönfeld P, Dymkowska D, Wojtczak L (2009) Acyl-CoA-induced generation of reactive oxygen species in mitochondrial preparations is due to the presence of peroxisomes. Free Radic Biol Med 47:503-9.
125. Schöpf B, Weissensteiner H, Schäfer G, et al (2020) OXPHOS remodeling in high-grade prostate cancer involves mtDNA mutations and increased succinate oxidation. Nat Commun 11:1487.
126. Schultz J, Wiesner RJ (2000) Proliferation of mitochondria in chronically stimulated rabbit skeletal muscle—transcription of mitochondrial genes and copy number of mitochondrial DNA. J Bioenerg Biomembr 32:627-34.
127. Simson P, Jepihhina N, Laasmaa M, et al (2016) Restricted ADP movement in cardiomyocytes: Cytosolic diffusion obstacles are complemented with a small number of open mitochondrial voltage-dependent anion channels. J Mol Cell Cardiol 97:197-203.
128. Singh BK, Sinha RA, Tripathi M, et al (2018) Thyroid hormone receptor and ERRα coordinately regulate mitochondrial fission, mitophagy, biogenesis, and function. Sci Signal 11(536) DOI: 10.1126/scisignal.aam5855.
129. Speijer D (2016) Being right on Q: shaping eukaryotic evolution. Biochem J 473:4103-27.
130. Stucki JW, Ineichen EA (1974) Energy dissipation by calcium recycling and the

efficiency of calcium transport in rat-liver mitochondria. Eur J Biochem 48:365-75.
131. Sugiura A, Mattie S, Prudent J, McBride HM (2017) Newly born peroxisomes are a hybrid of mitochondrial and ER-derived pre-peroxisomes. Nature 542:251-4.
132. Tonkonogi M, Harris B, Sahlin K (1997) Increased activity of citrate synthase in human skeletal muscle after a single bout of prolonged exercise. Acta Physiol Scand 161:435-6.
133. Torralba D, Baixauli F, Sánchez-Madrid F (2016) Mitochondria know no boundaries: mechanisms and functions of intercellular mitochondrial transfer. Front Cell Dev Biol 4:107. eCollection 2016.
134. Vamecq J, Schepers L, Parmentier G, Mannaerts GP (1987) Inhibition of peroxisomal fatty acyl-CoA oxidase by antimycin A. Biochem J 248:603-7.
135. Waczulikova I, Habodaszova D, Cagalinec M, et al (2007) Mitochondrial membrane fluidity, potential, and calcium transients in the myocardium from acute diabetic rats. Can J Physiol Pharmacol 85:372-81.
136. Wagner BA, Venkataraman S, Buettner GR (2011) The rate of oxygen utilization by cells. Free Radic Biol Med 51:700-712.
137. Wang H, Hiatt WR, Barstow TJ, Brass EP (1999) Relationships between muscle mitochondrial DNA content, mitochondrial enzyme activity and oxidative capacity in man: alterations with disease. Eur J Appl Physiol Occup Physiol 80:22-7.
138. Watt IN, Montgomery MG, Runswick MJ, et al (2010) Bioenergetic cost of making an adenosine triphosphate molecule in animal mitochondria. Proc Natl Acad Sci U S A 107:16823-7.
139. Weibel ER, Hoppeler H (2005) Exercise-induced maximal metabolic rate scales with muscle aerobic capacity. J Exp Biol 208:1635–44.
140. White DJ, Wolff JN, Pierson M, Gemmell NJ (2008) Revealing the hidden complexities of mtDNA inheritance. Mol Ecol 17:4925–42.
141. Wikström M, Hummer G (2012) Stoichiometry of proton translocation by respiratory complex I and its mechanistic implications. Proc Natl Acad Sci U S A 109:4431-6.
142. Williams EG, Wu Y, Jha P, et al (2016) Systems proteomics of liver mitochondria function. Science 352 (6291):aad0189
143. Willis WT, Jackman MR, Messer JI, et al (2016) A simple hydraulic analog model of oxidative phosphorylation. Med Sci Sports Exerc 48:990-1000.
144. Yoshinaga MY, Kellermann MY, Valentine DL, Valentine RC (2016) Phospholipids and glycolipids mediate proton containment and circulation along the surface of energy-transducing membranes. Prog Lipid Res 64:1-15.
145. Zíková A, Hampl V, Paris Z, et al (2016) Aerobic mitochondria of parasitic protists: diverse genomes and complex functions. Mol Biochem Parasitol 209:46-57.

*Authors — MitoEAGLE Task Group

Gnaiger Erich, Aasander Frostner Eleonor, Abdul Karim Norwahidah, Abdel-Rahman Engy Ali, Abumrad Nada A, Acuna-Castroviejo Dario, Adiele Reginald C, Ahn Bumsoo, Alencar Mayke Bezerra, Ali Sameh S, Almeida Angeles, Alton Lesley, Alves Marco G, Amati Francesca, Amoedo Nivea Dias, Amorim Ricardo, Anderson Ethan J, Andreadou Ioanna, Antunes Diana, Arago Marc, Aral Cenk, Arandarcikaite Odeta, Arias-Reyes Christian, Armand Anne-Sophie, Arnould Thierry, Avram Vlad F, Axelrod Christopher L, Bailey Damian M, Bairam Aida, Bajpeyi Sudip, Bajzikova Martina, Bakker Barbara M, Banni Aml, Bardal Tora, Barlow J, Bastos Sant'Anna Silva Ana Carolina, Batterson Philip M, Battino Maurizio, Bazil Jason N, Beard Daniel A, Bednarczyk Piotr, Beleza Jorge, Bello Fiona, Ben-Shachar Dorit, Bento Guida Jose Freitas, Bergdahl Andreas, Berge Rolf K, Bergmeister Lisa, Bernardi Paolo, Berridge Michael V, Bettinazzi Stefano, Bishop David J, Blier Pierre U, Blindheim Dan Filip, Boardman Neoma T, Boetker Hans Erik, Borchard Sabine, Boros Mihaly, Boersheim Elisabet, Borras Consuelo, Borutaite Vilma, Botella Javier, Bouillaud Frederic, Bouitbir Jamal, Boushel Robert C, Bovard Josh, Bravo-Sagua Roberto, Breton Sophie, Brown David A, Brown Guy C, Brown Robert Andrew, Brozinick Joseph T, Buettner Garry R, Burtscher Johannes, Bustos Matilde, Calabria Elisa, Calbet Jose AL, Calzia Enrico, Cannon Daniel T, Cano Sanchez Maria Consolacion, Canto Alvarez Carles, Cardinale Daniele A, Cardoso Luiza HD, Carvalho Eugenia, Casado Pinna Marta, Cassar Samantha, Castelo Rueda Maria Paulina, Castilho Roger F, Cavalcanti-de-Albuquerque Joao Paulo, Cecatto Cristiane, Celen Murat C, Cervinkova Zuzana, Chabi Beatrice, Chakrabarti Lisa, Chakrabarti Sasanka, Chaurasia Bhagirath, Chen Quan, Chicco Adam J, Chinopoulos

Christos, Chowdhury Subir Kumar, Cizmarova Beata, Clementi Emilio, Coen Paul M, Cohen Bruce H, Coker Robert H, Collin-Chenot Anne, Coughlan Melinda T, Coxito Pedro, Crisostomo Luis, Crispim Marcell, Crossland Hannah, Dahdah Norma Ramon, Dalgaard Louise T, Dambrova Maija, Danhelovska Tereza, Darveau Charles-A, Darwin Paula M, Das Anibh Martin, Dash Ranjan K, Davidova Eliska, Davis Michael S, Dayanidhi Sudarshan, De Bem Andreza Fabro, De Goede Paul, De Palma Clara, De Pinto Vito, Dela Flemming, Dembinska-Kiec Aldona, Detraux Damian, Devaux Yvan, Di Marcello Marco, Di Paola Floriana Jessica, Dias Candida, Dias Tania R, Diederich Marc, Distefano Giovanna, Djafarzadeh Siamak, Doermann Niklas, Doerrier Carolina, Dong Lan-Feng, Donnelly Chris, Drahota Zdenek, Duarte Filipe Valente, Dubouchaud Herve, Duchen Michael R, Dumas Jean-Francois, Durham William J, Dymkowska Dorota, Dyrstad Sissel E, Dyson Alex, Dzialowski Edward M, Eaton Simon, Ehinger Johannes K, Elmer Eskil, Endlicher Rene, Engin Ayse Basak, Escames Germaine, Evinova Andrea, Ezrova Zuzana, Falk Marni J, Fell David A, Ferdinandy Peter, Ferko Miroslav, Fernandez-Ortiz Marisol, Fernandez-Vizarra Erika, Ferreira Julio Cesar B, Ferreira Rita Maria P, Ferri Alessandra, Fessel Joshua Patrick, Festuccia William T, Filipovska Aleksandra, Fisar Zdenek, Fischer Christine, Fischer Michael J, Fisher Gordon, Fisher Joshua J, Fontanesi Flavia, Forbes-Hernandez Tamara Y, Ford Ellen, Fornaro Mara, Fuertes Agudo Marina, Fulton Montana, Galina Antonio, Galkin Alexander, Gallee Leon, Galli Gina L J, Gama Perez Pau, Gan Zhenji, Ganetzky Rebecca, Gao Yun, Garcia Geovana S, Garcia-Rivas Gerardo, Garcia-Roves Pablo Miguel, Garcia-Souza Luiz F, Garlid Keith D, Garrabou Gloria, Garten Antje, Gastaldelli Amalia, Gayen Jiaur, Genders Amanda J, Genova Maria Luisa, Giampieri Francesca, Giovarelli Matteo, Glatz Jan FC, Goikoetxea Usandizaga Naroa, Goncalo Teixeira da Silva Rui, Goncalves Debora Farina, Gonzalez-Armenta Jenny L, Gonzalez-Franquesa Alba, Gonzalez-Freire Marta, Gonzalo Hugo, Goodpaster Bret H, Gorr Thomas A, Gourlay Campbell W, Grams Bente, Granata Cesare, Grefte Sander, Grilo Luis, Guarch Meritxell Espino, Gueguen Naig, Gumeni Sentiljana, Haas Clarissa, Haavik Jan, Hachmo Yafit, Haendeler Judith, Haider Markus, Hajrulahovic Anesa, Hamann Andrea, Han Jin, Han Woo Hyun, Hancock Chad R, Hand Steven C, Handl Jiri, Hansikova Hana, Hardee Justin P, Hargreaves Iain P, Harper Mary-Ellen, Harrison David K, Hassan Hazirah, Hatokova Zuzana, Hausenloy Derek J, Heales Simon JR, Hecker Matthias, Heiestad Christina, Hellgren Kim T, Henrique Alexandrino, Hepple Russell T, Hernansanz-Agustin Pablo, Hewakapuge Sudinna, Hickey Anthony J, Ho Dieu Hien, Hoehn Kyle L, Hoel Fredrik, Holland Olivia J, Holloway Graham P, Holzner Lorenz, Hoppel Charles L, Hoppel Florian, Hoppeler Hans, Houstek Josef, Huete-Ortega Maria, Hyrossova Petra, Iglesias-Gonzalez Javier, Indiveri Cesare, Irving Brian A, Isola Raffaella, Iyer Shilpa, Jackson Christopher Benjamin, Jadiya Pooja, Jana Prado Fabian, Jandeleit-Dahm Karin, Jang David H, Jang Young Charles, Janowska Joanna, Jansen Kirsten M, Jansen-Duerr Pidder, Jansone Baiba, Jarmuszkiewicz Wieslawa, Jaskiewicz Anna, Jaspers Richard T, Jedlicka Jan, Jerome Estaquier, Jespersen Nichlas Riise, Jha Rajan Kumar, Jones John G, Joseph Vincent, Juhasz Laszlo, Jurczak Michael J, Jurk Diana, Jusic Amela, Kaambre Tuuli, Kaczor Jan Jacek, Kainulainen Heikki, Kampa Rafal Pawel, Kandel Sunil Mani, Kane Daniel A, Kapferer Werner, Kapnick Senta, Kappler Lisa, Karabatsiakis Alexander, Karavaeva Iuliia, Karkucinska-Wieckowska Agnieszka, Kaur Sarbjot, Keijer Jaap, Keller Markus A, Keppner Gloria, Khamoui Andy V, Kidere Dita, Kilbaugh Todd, Kim Hyoung Kyu, Kim Julian KS, Kimoloi Sammy, Klepinin Aleksandr, Klepinina Lyudmila, Klingenspor Martin, Klocker Helmut, Kolassa Iris, Komlodi Timea, Koopman Werner JH, Kopitar-Jerala Natasa, Kowaltowski Alicia J, Kozlov Andrey V, Krajcova Adela, Krako Jakovljevic Nina, Kristal Bruce S, Krycer James R, Kuang Jujiao, Kucera Otto, Kuka Janis, Kwak Hyo Bum, Kwast Kurt E, Kwon Oh Sung, Laasmaa Martin, Labieniec-Watala Magdalena, Lagarrigue Sylviane, Lai Nicola, Lalic Nebojsa M, Land John M, Lane Nick, Laner Verena, Lanza Ian R, Laouafa Sofien, Laranjinha Joao, Larsen Steen, Larsen Terje S, Lavery Gareth G, Lazou Antigone, Ledo Ana Margarida, Lee Hong Kyu, Leeuwenburgh Christiaan, Lehti Maarit, Lemieux Helene, Lenaz Giorgio, Lerfall Joergen, Li Pingan Andy, Li Puma Lance, Liang Liping, Liepins Edgars, Lin Chien-Te, Liu Jiankang, Lopez Garcia Luis Carlos, Lucchinetti Eliana, Ma Tao, Macedo Maria Paula, Machado Ivo F, Maciej Sarah, MacMillan-Crow Lee Ann, Magalhaes Jose, Magri Andrea, Majtnerova Pavlina, Makarova Elina, Makrecka-Kuka Marina, Malik Afshan N, Marcouiller Francois, Marechal Amandine, Markova Michaela, Markovic Ivanka, Martin Daniel S, Martins Ana Dias, Martins Joao D, Maseko Tumisang Edward, Maull Felicia, Mazat Jean-Pierre, McKenna Helen T, McKenzie Matthew, McMillan Duncan GG, McStay Gavin P, Mendham Amy, Menze Michael A, Mercer John R, Merz Tamara, Messina Angela, Meszaros Andras, Methner Axel, Michalak Slawomir, Mila Guasch Maria, Minuzzi Luciele M, Misirkic Marjanovic Maja, Moellering Douglas R, Moisoi Nicoleta, Molina Anthony JA, Montaigne David, Moore Anthony L, Moore Christy, Moreau Kerrie, Moreira Bruno P, Moreno-Sanchez Rafael, Mracek Tomas, Muccini Anna Maria, Munro Daniel, Muntane Jordi, Muntean Danina M, Murray Andrew James, Musiol Eva, Nabben Miranda, Nair K Sreekumaran, Nehlin Jan O, Nemec Michal, Nesci Salvatore, Neufer P Darrell, Neuzil Jiri, Neviere Remi, Newsom Sean A, Norman Jennifer, Nozickova Katerina, Nunes Sara, Nuoffer Jean-Marc, O'Brien Kristin, O'Brien Katie A, O'Gorman Donal, Olgar Yusuf, Oliveira Ben, Oliveira Jorge, Oliveira Marcus F, Oliveira Marcos Tulio, Oliveira Pedro Fontes, Oliveira Paulo J, Olsen Rolf Erik, Orynbayeva Zulfiya, Osiewacz Heinz D, Paez Hector, Pak Youngmi Kim, Pallotta Maria Luigia, Palmeira Carlos, Parajuli Nirmala, Passos Joao F, Passrugger Manuela, Patel Hemal H, Pavlova Nadia, Pavlovic Kasja, Pecina Petr, Pedersen Tina M, Perales Jose Carles, Pereira da Silva Grilo da Silva Filomena, Pereira Rita, Pereira Susana P, Perez Valencia Juan Alberto, Perks Kara L, Pesta Dominik, Petit Patrice X, Pettersen Nitschke Ina Katrine, Pichaud Nicolas, Pichler Irene, Piel Sarah, Pietka Terri A, Pinho Sonia A, Pino Maria F, Pirkmajer Sergej, Place Nicolas, Plangger Mario, Porter Craig, Porter Richard K, Preguica Ines, Prigione Alessandro, Procaccio Vincent, Prochownik Edward V, Prola Alexandre, Pulinilkunnil Thomas, Puskarich Michael A, Puurand Marju, Radenkovic Filip, Ramzan Rabia, Rattan Suresh IS, Reano Simone, Reboredo-Rodriguez Patricia, Rees Bernard B, Renner-Sattler Kathrin, Rial Eduardo, Robinson Matthew M, Roden Michael, Rodrigues Ana Sofia, Rodriguez Enrique, Rodriguez-Enriquez Sara, Roesland Gro Vatne, Rohlena Jakub, Rolo Anabela Pinto, Ropelle Eduardo R, Roshanravan Baback, Rossignol Rodrigue, Rossiter Harry B, Rousar Tomas, Rubelj Ivica, Rybacka-Mossakowska Joanna, Saada Reisch Ann, Safaei Zahra, Salin Karine, Salvadego Desy, Sandi Carmen, Saner Nicholas, Santos Diana, Sanz Alberto, Sardao Vilma, Sarlak Saharnaz, Sazanov Leonid A, Scaife Paula, Scatena Roberto, Schartner Melanie, Scheibye-Knudsen Morten, Schilling Jan M, Schlattner Uwe, Schmitt Sabine, Schneider Gasser Edith Mariane, Schoenfeld Peter, Schots Pauke C, Schulz Rainer, Schwarzer Christoph, Scott Graham R, Selman Colin, Sendon Pamella Marie, Shabalina Irina G, Sharma Pushpa, Sharma Vipin, Shevchuk Igor, Shirazi Reza, Shiroma Jonathan G, Siewiera Karolina, Silber Ariel Mariano, Silva Ana Maria, Sims Carrie A, Singer Dominique, Singh Brijesh Kumar, Skolik Robert A, Smenes Benedikte Therese, Smith James, Soares Felix Alexandre Antunes, Sobotka Ondrej, Sokolova Inna, Solesio Maria E, Soliz Jorge, Sommer Natascha, Sonkar Vijay K, Sova Marina, Sowton Alice P, Sparagna Genevieve C, Sparks Lauren M, Spinazzi Marco, Stankova Pavla, Starr Jonathan, Stary Creed, Stefan Eduard, Stelfa Gundega, Stepto Nigel K, Stevanovic Jelena, Stiban Johnny, Stier Antoine, Stocker Roland, Storder Julie, Sumbalova Zuzana, Suomalainen Anu, Suravajhala Prashanth, Svalbe Baiba, Swerdlow Russell H, Swiniuch Daria, Szabo Ildiko, Szewczyk Adam, Szibor Marten, Tanaka Masashi, Tandler Bernard, Tarnopolsky Mark A, Tausan Daniel, Tavernarakis Nektarios, Teodoro Joao Soeiro, Tepp Kersti, Thakkar Himani, Thapa Maheshwor, Thyfault John P, Tomar Dhanendra, Ton Riccardo, Torp May-Kristin, Torres-Quesada Omar, Towheed Atif, Treberg Jason R, Tretter Laszlo, Trewin Adam J, Trifunovic Aleksandra, Trivigno Catherine, Tronstad Karl Johan, Trougakos Ioannis P, Truu Laura, Tuncay Erkan, Turan Belma, Tyrrell Daniel J, Urban Tomas, Urner

Sofia, Valentine Joseph Marco, Van Bergen Nicole J, Van der Ende Miranda, Varricchio Frederick, Vaupel Peter, Vella Joanna, Vendelin Marko, Vercesi Anibal E, Verdaguer Ignasi Bofill, Vernerova Andrea, Victor Victor Manuel, Vieira Ligo Teixeira Camila, Vidimce Josif, Viel Christian, Vieyra Adalberto, Vilks Karlis, Villena Josep A, Vincent Vinnyfred, Vinogradov Andrey D, Viscomi Carlo, Vitorino Rui Miguel Pinheiro, Vlachaki Walker Julia, Vogt Sebastian, Volani Chiara, Volska Kristine, Votion Dominique-Marie, Vujacic-Mirski Ksenija, Wagner Brett A, Ward Marie Louise, Warnsmann Verena, Wasserman David H, Watala Cezary, Wei Yau-Huei, Weinberger Klaus M, Weissig Volkmar, White Sarah Haverty, Whitfield Jamie, Wickert Anika, Wieckowski Mariusz R, Wiesner Rudolf J, Williams Caroline M, Winwood-Smith Hugh, Wohlgemuth Stephanie E, Wohlwend Martin, Wolff Jonci Nikolai, Wrutniak-Cabello Chantal, Wuest Rob CI, Yokota Takashi, Zablocki Krzysztof, Zanon Alessandra, Zanou Nadege, Zaugg Kathrin, Zaugg Michael, Zdrazilova Lucie, Zhang Yong, Zhang Yizhu, Zikova Alena, Zischka Hans, Zorzano Antonio, Zujovic Tijana, Zurmanova Jitka, Zvejniece Liga

Affiliations:
https://www.bioenergetics-communications.org/index.php/BEC_2020.1_doi10.26124bec2020-0001.v1

Author contributions: This manuscript developed as an open invitation to scientists and students to join as coauthors in the bottom-up spirit of COST, based on a first draft written by the corresponding author, who integrated coauthor contributions in a sequence of Open Access versions. Coauthors contributed to the scope and quality of the manuscript, may have focused on a particular section, and are listed in alphabetical order. Coauthors confirm that they have read the final manuscript and agree to implement or discuss the recommendations in future manuscripts, presentations and teaching materials.

Acknowledgements: We thank Marija Beno for management assistance, and Peter R Rich for valuable discussions. This publication is based upon work from COST Action CA15203 MitoEAGLE, supported by COST (European Cooperation in Science and Technology), in cooperation with COST Actions CA16225 EU-CARDIOPROTECTION and CA17129 CardioRNA; K-Regio project MitoFit funded by the Tyrolian Government, and project NextGen-O2k which has received funding from the European Union's Horizon 2020 research and innovation programme under grant agreement No. 859770.

Funded by the Horizon 2020 Framework Programme of the European Union

COST Action CA15203 **MitoEAGLE**

Competing financial interests: Erich Gnaiger is founder and CEO of Oroboros Instruments, Innsbruck, Austria.

Corresponding author: Erich Gnaiger
Chair COST Action CA15203 MitoEAGLE
http://www.mitoeagle.org
Department of Visceral, Transplant and Thoracic Surgery, D. Swarovski Research Laboratory, Medical University of Innsbruck, Innrain 66/4, A-6020 Innsbruck, Austria
Email: mitoeagle@i-med.ac.at
Tel +43 512 566796, Fax +43 512 566796 20

Published online: 2020-05-20

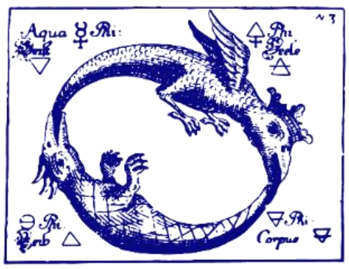

BIOENERGETICS COMMUNICATIONS